



**HAL**  
open science

## Penicillin-binding protein folding is dependent on the PrsA peptidyl-prolyl cis-trans isomerase in *Bacillus subtilis*

Hanne-Leena Hyyryläinen, Bogumila C. Marciniak, Kathleen Dahncke, Milla Pietiäinen, Pascal Courtin, Marika Vitikainen, Raili Seppala, Andreas Otto, Dörte Becher, Marie-Pierre Chapot-Chartier, et al.

### ► To cite this version:

Hanne-Leena Hyyryläinen, Bogumila C. Marciniak, Kathleen Dahncke, Milla Pietiäinen, Pascal Courtin, et al.. Penicillin-binding protein folding is dependent on the PrsA peptidyl-prolyl cis-trans isomerase in *Bacillus subtilis*. *Molecular Microbiology*, 2010, 10.1111/j.1365-2958.2010.07188.x . hal-00552636

**HAL Id: hal-00552636**

**<https://hal.science/hal-00552636>**

Submitted on 6 Jan 2011

**HAL** is a multi-disciplinary open access archive for the deposit and dissemination of scientific research documents, whether they are published or not. The documents may come from teaching and research institutions in France or abroad, or from public or private research centers.

L'archive ouverte pluridisciplinaire **HAL**, est destinée au dépôt et à la diffusion de documents scientifiques de niveau recherche, publiés ou non, émanant des établissements d'enseignement et de recherche français ou étrangers, des laboratoires publics ou privés.

**Penicillin-binding protein folding is dependent on the PrsA  
peptidyl-prolyl *cis-trans* isomerase in *Bacillus subtilis***

Journal:	<i>Molecular Microbiology</i>
Manuscript ID:	MMI-2010-09903.R1
Manuscript Type:	Research Article
Date Submitted by the Author:	16-Apr-2010
Complete List of Authors:	<p>Hyyryläinen, Hanne-Leena; National Institute for Health and Welfare, Department of Infectious Disease Surveillance and Control          Marciniak, Bogumila; University of Groningen, Department of Molecular Genetics          Dahncke, Kathleen; Ernst-Moritz-Arndt-University, Institute of Microbiology          Pietiäinen, Milla; National Institute for Health and Welfare, Department of Infectious Disease Surveillance and Control          Courtin, Pascal; INRA, Microbiology          Vitikainen, Marika; National Institute for Health and Welfare, Department of Infectious Disease Surveillance and Control          Seppala, Raili; National Institute for Health and Welfare, Department of Infectious Disease Surveillance and Control          Otto, Andreas; Ernst-Moritz-Arndt-University, Institute of Microbiology          Becher, Dörte; Ernst-Moritz-Arndt-University, Institute of Microbiology          Chapot-Chartier, Marie-Pierre; INRA, Microbiology          Kuipers, Oscar; University of Groningen, Department of Molecular Genetics          Kontinen, Vesa; National Institute for Health and Welfare, Department of Infectious Disease Surveillance and Control</p>
Key Words:	parvulin, peptidoglycan biosynthesis, bacterial cell wall, protein folding, antimicrobial drug target

1  
2  
3  
4  
5  
6  
7  
8  
9  
10  
11  
12  
13  
14  
15  
16  
17  
18  
19  
20  
21  
22  
23  
24  
25

## **Penicillin-binding protein folding is dependent on the PrsA peptidyl-prolyl *cis-trans* isomerase in *Bacillus subtilis***

Hanne-Leena Hyyryläinen<sup>1</sup>, Bogumila C. Marciniak<sup>2</sup>, Kathleen Dahncke<sup>3¶</sup>, Milla Pietiäinen<sup>1</sup>, Pascal Courtin<sup>4</sup>, Marika Vitikainen<sup>1†</sup>, Raili Seppälä<sup>1</sup>, Andreas Otto<sup>3</sup>, Dörte Becher<sup>3</sup>, Marie-Pierre Chartier<sup>4</sup>, Oscar P. Kuipers<sup>2</sup>, Vesa P. Kontinen<sup>1\*</sup>

<sup>1</sup> Antimicrobial Resistance Unit, Department of Infectious Disease Surveillance and Control, National Institute for Health and Welfare (THL), P.O. Box 30, FI-00271 Helsinki, Finland.

<sup>2</sup> Molecular Genetics Group, Groningen Biomolecular Sciences and Biotechnology Institute, University of Groningen, Kerklaan 30, 9751 NN Haren, the Netherlands.

<sup>3</sup> Institut für Mikrobiologie, Ernst-Moritz-Arndt Universität Greifswald, Friedrich-Ludwig-Jahn-Str. 15, D-17489 Greifswald, Germany.

<sup>4</sup> INRA, UR477 Biochimie Bactérienne, F-78350 Jouy-en-Josas, France.

Correspondence to \*E-mail [vesa.kontinen@thl.fi](mailto:vesa.kontinen@thl.fi); Tel. (+358) 20 610 68562; Fax. (+358) 20 610 68238.

E-mail addresses, telephone and fax numbers of the authors:

HLH: E-mail [hanne-leena.hyyrylainen@thl.fi](mailto:hanne-leena.hyyrylainen@thl.fi); Tel. (+358) 20 610 8417; Fax. (+358) 20 610 8238

BCM: E-mail [b.c.marciniak@rug.nl](mailto:b.c.marciniak@rug.nl); Tel. (+31) 50 3632093; Fax. (+31) 50 3632348

KD: E-mail [kathleen.dahncke@fu-berlin.de](mailto:kathleen.dahncke@fu-berlin.de); Tel. (+49) 30 838 55431; Fax. (+49) 30 838 53372

MP: E-mail [milla.pietiainen@thl.fi](mailto:milla.pietiainen@thl.fi); Tel. 020 610 8880; Fax. (+358) 20 610 8238

PC: Email [Pascal.Courtin@jouy.inra.fr](mailto:Pascal.Courtin@jouy.inra.fr); Tel. (+33) 1 34 65 22 68; Fax. (+33) 1 34 65 21 63

- 26 MV: Email [marika.vitikainen@vtt.fi](mailto:marika.vitikainen@vtt.fi); Tel. (+358) 20 722 4031; Fax. (+358) 20 722 7071
- 27 RS: E-mail [rsseppal@mappi.helsinki.fi](mailto:rsseppal@mappi.helsinki.fi); Tel. (+358) 50 5739161
- 28 AO: E-mail [andreas.otto@uni-greifswald.de](mailto:andreas.otto@uni-greifswald.de); Tel. (+49) 3834 864230; (+49) 3834 864202.
- 29 DB: E-mail [dbecher@uni-greifswald.de](mailto:dbecher@uni-greifswald.de); Tel. (+49) 3834 864230; Fax. (+49) 3834 864202
- 30 PPCC: Email [Marie-Pierre.Chapot@jouy.inra.fr](mailto:Marie-Pierre.Chapot@jouy.inra.fr); Tel. (+33) 1 34 65 22 68; Fax. (+33) 1 34 65 21 63
- 31 OPK: E-mail [o.p.kuipers@rug.nl](mailto:o.p.kuipers@rug.nl); Tel. (+31) 50 3632093; Fax. (+31) 50 3632348
- 32 VPK: E-mail [vesa.kontinen@thl.fi](mailto:vesa.kontinen@thl.fi); Tel. (+358) 20 610 68562; Fax. (+358) 20 610 68238

33

34 Present addresses:

35 ¶ Abteilung Biochemie der Pflanzen, Institut für Biologie, Freie Universität Berlin, Königin-Luise-  
36 Straße 12-16, D-14195 Berlin, Germany

37 † VTT Technical Research Centre of Finland, Biotechnology, Tietotie 2, Espoo, P.O. Box 1000, FI-  
38 02044 VTT, Finland

39

40 Running title: PrsA PPIase for penicillin-binding protein folding

41

42 Key words: parvulin, peptidoglycan biosynthesis, bacterial cell wall, protein folding, antimicrobial  
43 drug target

44

45

46

47

48

49

50 **SUMMARY**

51

52 The PrsA protein is a membrane-anchored peptidyl-prolyl *cis-trans* isomerase in *Bacillus subtilis*  
53 and most other gram-positive bacteria. It catalyzes the post-translocational folding of exported  
54 proteins and is essential for normal growth of *B. subtilis*. We studied the mechanism behind this  
55 indispensability. We could construct a viable *prsA* null mutant in the presence of a high  
56 concentration of magnesium. Various changes in cell morphology in the absence of PrsA suggested  
57 that PrsA is involved in the biosynthesis of the cylindrical lateral wall. Consistently, four penicillin-  
58 binding proteins (PBP2a, PBP2b, PBP3 and PBP4) were unstable in the absence of PrsA, while  
59 mucopeptide analysis revealed a 2% decrease in the peptidoglycan crosslinkage index. Misfolded  
60 PBP2a was detected in PrsA-depleted cells, indicating that PrsA is required for the folding of this  
61 PBP either directly or indirectly. Furthermore, strongly increased uniform staining of cell wall with  
62 a fluorescent vancomycin was observed in the absence of PrsA. We also demonstrated that PrsA is  
63 a dimeric or oligomeric protein which is localized at distinct spots organized in a helical pattern  
64 along the cell membrane. These results suggest that PrsA is essential for normal growth most  
65 probably since PBP folding is dependent on this PPIase.

66

67

68

69

70 **INTRODUCTION**

71

72 Intracellular folding of a protein into a native functional structure is assisted by molecular  
73 chaperones and foldase enzymes. A class of foldases ubiquitous in all types of cells and cell  
74 compartments is formed by peptidyl-prolyl *cis-trans* isomerases (PPIases), which catalyze the  
75 isomerization of peptide bonds immediately preceding proline residues (Schiene and Fischer, 2000,  
76 Wang and Heitman, 2005, Lu and Zhou, 2007). Three families of PPIases have been identified:  
77 cyclophilins, FK506-binding proteins and parvulins (Rahfeld *et al.*, 1994). The archetype of the  
78 parvulin family of PPIases is the *Escherichia coli* Par10, which consists of 92 amino acid residues  
79 comprising the minimal catalytic domain (Kühlewein *et al.*, 2004). In other parvulins, a catalytic  
80 domain is flanked with N- and C- terminal regions of various lengths and roles in substrate binding  
81 and/or chaperone-like catalysis of folding (Lu *et al.*, 1996, Yaffe *et al.*, 1997, Uchida *et al.*, 1999,  
82 Wu *et al.*, 2000, Behrens *et al.*, 2001, Vitikainen *et al.*, 2004). Human Pin1 and its counterpart  
83 parvulins in other eukaryotic cells specifically recognize proline residues that are preceded by  
84 phosphorylated serine or threonine residues (Hani *et al.*, 1999, Lu *et al.*, 1999, Yao *et al.*, 2001, Lu  
85 and Zhou, 2007). Other parvulins have a wider substrate range, since their substrate recognition is  
86 independent of phosphorylation (Hennecke *et al.*, 2005, Stymest and Klappa, 2008).

87

88 PrsA is a lipoprotein bound to the outer face of the cytoplasmic membrane in *Bacillus subtilis* and  
89 other gram-positive Firmicutes (Kontinen and Sarvas, 1993, Vitikainen *et al.*, 2004). It consists of a  
90 diacylglycerol membrane anchor, a large functionally unknown N-terminal domain followed by a  
91 PPIase domain with similarity to the parvulin family of PPIases and a small functionally unknown  
92 C-terminal domain (Vitikainen *et al.*, 2004). *B. subtilis* PrsA exhibits PPIase activity but may also  
93 have a chaperone-like activity *in vivo* (Vitikainen *et al.*, 2004). The presence of a deletion in the

94 PPIase domain of the *Lactococcus lactis* PrsA-like protein PmpA suggests that it may function only  
95 as a chaperone (Drouault *et al.*, 2002). The periplasmic SurA of *Escherichia coli* is also a chaperone  
96 with a specialized role in the folding and assembly of outer-membrane proteins (Behrens *et al.*,  
97 2001). Several extracellular proteins in various gram-positive bacteria are secreted or matured in a  
98 PrsA-dependent manner (Kontinen and Sarvas, 1993, Hyyryläinen *et al.*, 2000, Vitikainen *et al.*,  
99 2001, Drouault *et al.*, 2002, Vitikainen *et al.*, 2005, Lindholm *et al.*, 2006, Ma *et al.*, 2006, Alonzo  
100 *et al.*, 2009, Zemansky *et al.*, 2009). Overexpression of PrsA enhances  $\alpha$ -amylase secretion from  
101 *Bacillus* and *Lactococcus lactis* cells (Kontinen and Sarvas, 1993, Vitikainen *et al.*, 2001,  
102 Vitikainen *et al.*, 2005, Lindholm *et al.*, 2006) including the biotechnically important  
103 thermoresistant AmyL  $\alpha$ -amylase of *Bacillus licheniformis* (Kontinen and Sarvas, 1993). Some  
104 other extracellular proteins are also secreted at increased levels from PrsA-overexpressing cells (Wu  
105 *et al.*, 1998, Williams *et al.*, 2003). In *B. subtilis*, PrsA is an essential cell component in normal  
106 growth conditions indicating that it has an indispensable role in protein folding at the membrane-  
107 cell wall interface (“periplasm”) (Vitikainen *et al.*, 2001). All three domains are essential for PrsA  
108 function (Vitikainen *et al.*, 2004). Inactivation of the D-alanylation system of the teichoic acids  
109 (Dlt) restores slight growth of *B. subtilis* cells lacking PrsA, suggesting that the increased net  
110 negative charge of the wall in the absence of Dlt partially suppresses the growth defect  
111 (Hyyryläinen *et al.*, 2000). In contrast to the rod-shaped *B. subtilis*, PrsA is a dispensable protein in  
112 several cocci, *Lactococcus lactis* (Drouault *et al.*, 2002), *Streptococcus pyogenes* (Ma *et al.*, 2006)  
113 and *Staphylococcus aureus* (Vitikainen *et al.*, unpublished).

114

115 In this study our purpose was to identify the indispensable cell component(s) which is (are) folded  
116 in a PrsA-dependent manner and to elucidate why PrsA is an essential protein in the rod-shaped  
117 bacterium *B. subtilis*, but non-essential in cocci. A hypothesis explaining this difference could be  
118 that PrsA catalyzes the folding of a protein(s) involved in the biosynthesis of the cylindrical (lateral)

119 cell wall and determination of the rod cell shape. The bacterial cell shape is maintained by a  
120 peptidoglycan cell wall (murein sacculus) and the actin-like proteins Mbl, MreB and MreBH, which  
121 form helical cables (cytoskeleton) that encircle the cell immediately beneath the cell membrane  
122 (Jones *et al.*, 2001, Carballido-Lopez and Errington, 2003, Soufo and Graumann, 2003, Defeu  
123 Soufo and Graumann, 2004, Stewart, 2005, Kawai *et al.*, 2009). The rod shape of *B. subtilis* is also  
124 dependent on other proteins including MreC and MreD, which are membrane proteins and interact  
125 with each other and Mbl (Defeu Soufo and Graumann, 2006, van den Ent *et al.*, 2006). In the  
126 absence of any of these Mre proteins, cells are spherical or aberrant in shape or non-viable in  
127 normal growth conditions (Jones *et al.*, 2001, Leaver and Errington, 2005, Kawai *et al.*, 2009).  
128 Studies on the cell shape determination of *Caulobacter crescentus* and *B. subtilis* have also shown  
129 that MreB, MreC and MreD interact with penicillin-binding proteins (PBPs) (Figge *et al.*, 2004,  
130 Divakaruni *et al.*, 2005, van den Ent *et al.*, 2006, Kawai *et al.*, 2009). Peptidoglycan precursors are  
131 incorporated into the wall at distinct sites organized in a helical pattern along the lateral wall  
132 (Daniel and Errington, 2003, Tiyanont *et al.*, 2006, Divakaruni *et al.*, 2007). The Mre proteins and  
133 two PBP1-associated cell division proteins, EzrA and GpsB, are involved in the determination of  
134 the spatial organization and dynamics of the peptidoglycan synthesis (Claessen *et al.*, 2008, Kawai  
135 *et al.*, 2009). In *Corynebacterium glutamicum*, which does not have the *mreB* gene (Daniel and  
136 Errington, 2003), peptidoglycan precursors are incorporated for the whole lateral wall via the newly  
137 formed division poles. In *Staphylococcus aureus* and probably in cocci more generally,  
138 peptidoglycan synthesis takes place only at the division septum and the hemispherical poles derived  
139 from it after cell division (Pinho and Errington, 2003).

140

141 High-molecular-weight penicillin-binding proteins are membrane-bound transglycosylase and  
142 transpeptidase enzymes which use peptidoglycan precursors to synthesize peptidoglycan chains and  
143 cross-link adjacent glycan chains to form a murein sacculus (Popham and Young, 2003, Sauvage *et*

144 *al.*, 2008). Class A high-molecular-weight PBPs possess both transglycosylase and transpeptidase  
145 activities, whereas class B high-molecular-weight PBPs have only transpeptidase activity (Scheffers  
146 *et al.*, 2004). In addition to these two classes of high-molecular-weight PBPs, bacterial cells also  
147 contain low-molecular-weight PBPs (class C) which have neither transglycosylase nor  
148 transpeptidase activity, but function as carboxypeptidases or endopeptidases (Popham and Young,  
149 2003, Sauvage *et al.*, 2008). The *B. subtilis* genome sequence has revealed 16 PBP-encoding genes,  
150 many of which are functionally redundant (Scheffers *et al.*, 2004). The PBPs have several distinct  
151 localization patterns in the cell suggesting dedicated functional roles for them in cell wall growth or  
152 cell division (Scheffers *et al.*, 2004). The PBP3 and PBP4a monofunctional transpeptidases and the  
153 PBP5 D-alanyl-D-alanine carboxypeptidase are localized in distinct spots or bands in the region of  
154 the lateral cell wall, suggesting their involvement in the elongation of the lateral wall. The  
155 bifunctional PBP1 is involved in the growth of both the lateral wall and the septum (Pedersen *et al.*,  
156 1999, Scheffers *et al.*, 2004, Claessen *et al.*, 2008, Kawai *et al.*, 2009). The PBP2a and PbpH  
157 transpeptidases have a redundant, essential activity in the lateral wall synthesis and rod-shape  
158 determination (Wei *et al.*, 2003), whereas the septal localization of PBP2b suggests a specific role  
159 for this transpeptidase in cell division (Scheffers *et al.*, 2004).

160

161 MreC and PBPs possess a number of proline residues (about 3% of amino acid residues) and the  
162 functional domains of these proteins are localized in the same cell compartment as PrsA suggesting  
163 that their folding could be dependent on PrsA. Misfolded proteins are rapidly degraded by the  
164 quality-control proteases such as HtrA (Hyryläinen *et al.*, 2001). We studied the stability of MreC  
165 and PBPs in cells depleted of PrsA to find out whether misfolding of these proteins occurs in the  
166 absence of PrsA. Stabilities of three divisome proteins with a “periplasmic” domain, FtsL, DivIB  
167 and DivIC (Daniel *et al.*, 1998, Katis and Wake, 1999) were also determined in a similar manner.  
168 Membrane proteomes were analyzed to identify other possible PrsA-dependent membrane proteins.

169 Various methods and approaches including electron microscopy, mucopeptide analysis and labeling  
170 of PBPs and peptidoglycan precursors with fluorescent antibiotics were used to characterize the cell  
171 wall biosynthesis defect of PrsA-depleted cells and the functional role of PrsA in cell shape  
172 determination. Furthermore, we studied whether PrsA is evenly or non-evenly distributed along the  
173 cell membrane. The results showed that several PBPs are folded in a PrsA-dependent manner,  
174 suggesting that this is the likely cause for the growth arrest in the absence of PrsA.

For Peer Review

175

176 **RESULTS**

177

178 *B. subtilis* cells depleted of the PrsA protein are able to grow in the presence of a high  
179 concentration of magnesium

180

181 In order to modulate cellular amount of PrsA, we have placed the *B. subtilis prsA* gene under the  
182 transcriptional control of the IPTG-inducible *Pspac* promoter (Vitikainen *et al.*, 2001).  
183 Transmission electron microscope images of cells expressing *Pspac-prsA* (IH7211) at low levels  
184 showed that PrsA depletion causes distinct changes in cell morphology. Severely PrsA-depleted  
185 cells which were still able to grow (*Pspac-prsA* induced with 8  $\mu$ M IPTG) were rod shaped but  
186 much larger than cells of the parental wild-type strain (compare Fig. 1A and 1B). At a PrsA level  
187 that was insufficient to support normal growth, large spherical cells were observed (Fig. 1C-D).  
188 Thick cell wall material was seen in residual division septa between the spherical cells, whereas in  
189 the periphery in many sites only a thin wall layer was left, suggesting that PrsA may be required for  
190 the biosynthesis of the lateral cell wall. These changes in cell morphology are similar to those seen  
191 in defects of the cell wall polymer biosynthesis and cell shape determination (Wei *et al.*, 2003,  
192 Leaver and Errington, 2005).

193

194 The MreC and MreD cell shape-determination proteins are required for lateral cell wall biosynthesis  
195 and normal growth of *B. subtilis*. However, a high concentration of magnesium (20 mM) in the  
196 growth medium restores some growth even in the complete absence of these proteins (Leaver and  
197 Errington, 2005). Cells depleted of MreC or MreD in the presence of 20 mM magnesium are  
198 spherical in shape. The mechanism of this suppression is currently unknown. Since magnesium also  
199 rescues growth of other mutants with defects in different aspects of cell wall biosynthesis ( $\Delta$ *ponA*

200 and  $\Delta mreB$ ), and which in contrast to *mreC* and *mreD* mutants maintain a wild type-like rod shape,  
201 it may affect indirectly peptidoglycan structure or turnover (Formstone and Errington, 2005). We  
202 studied whether the growth defect of PrsA-depleted cells can be suppressed by magnesium. The  
203 strain IH7211 (*Pspac-prsA*) was grown in Antibiotic Medium 3 in the presence or absence of IPTG  
204 and the effect of 20 mM  $MgCl_2$  on the growth was determined. Interestingly, magnesium restored  
205 the growth of PrsA-depleted IH7211 (Fig. 2). However, even though the PrsA-depleted cells grew  
206 in the presence of magnesium, it did not restore the “normal” morphology of PrsA-expressing cells  
207 but they remained thick rods (Fig. 1E-F).

208  
209 *PrsA is required for the stability of several penicillin-binding proteins*

210  
211 The above results suggest that PrsA is involved in the folding of a membrane protein(s) which has  
212 (have) a large “periplasmic” domain with an essential role(s) in the wall biosynthesis and/or cell  
213 shape determination. We used N-terminal green fluorescence protein (GFP) tags and specific  
214 antibodies against GFP, MreC and PrsA to determine effects of the PrsA depletion on the stability  
215 of potential PrsA-dependent membrane components. We started this study with GFP fusions, since  
216 most of these constructs were available and used previously in other studies (Scheffers *et al.*, 2004,  
217 Leaver and Errington, 2005). We were particularly interested in finding out whether the stability of  
218 MreC and penicillin-binding proteins (PBPs) is dependent on PrsA. The penicillin-binding protein  
219 2b (PBP2b) interacts with the divisome proteins DivIB, DivIC and FtsL and affects their stability  
220 (Daniel *et al.*, 2006). Furthermore, an NMR study of DivIB suggested that *cis-trans* isomerization  
221 of a specific prolyl peptide bond causes a major structural change in this divisome protein and it  
222 was proposed that the *cis-trans* isomerisation may function as a regulatory switch in cell division  
223 (Robson and King, 2006). Therefore, we were also interested in determining the stability of DivIB,  
224 DivIC and FtsL in PrsA-depleted cells.

225

226 The absence of PrsA did not decrease cellular levels of MreC and GFP-MreC as determined by  
227 immunoblotting with anti-MreC antibodies, suggesting that PrsA is not essential for the folding and  
228 stability of this cell shape-determination protein (Fig. S1). Hence, despite of the similar suppression  
229 of the growth defects of PrsA-depleted and MreC-depleted cells by magnesium, the growth  
230 inhibition in the absence of PrsA is most probably not caused by misfolding of MreC. In contrast,  
231 PBP2a, a high-molecular-weight penicillin-binding protein, which is involved in the lateral cell wall  
232 biosynthesis (Wei *et al.*, 2003), is most probably a PrsA-dependent protein, as indicated by a clear  
233 decrease in the level of GFP-PBP2a in PrsA-depleted cells expressing this fusion protein (Fig. 3A)  
234 and in their isolated membranes (Fig. S1). The PrsA dependency of PBP1a/b, the largest of the  
235 penicillin-binding proteins of *B. subtilis*, was also studied with a GFP-PBP1a/b construct. GFP-  
236 PBP1a/b was stable in PrsA-depleted cells (Fig. S1), suggesting that PBP1a/b folding is  
237 independent of PrsA. The PrsA-dependency analysis of the DivIB, DivIC and FtsL divisome  
238 proteins revealed that none of them are PrsA dependent (Fig. S2).

239

240 The binding of  $\beta$ -lactam antibiotics to the native fold of PBPs can be used to visualize and  
241 determine cellular levels of enzymatically-active PBPs. In order to elucidate the effect of the PrsA  
242 depletion on the levels of correctly-folded PBPs, cell membranes were isolated from PrsA-depleted  
243 and non-depleted cells and PBPs were labeled with fluorescent penicillin, Bocillin-FL, and analyzed  
244 with SDS-PAGE. There are sixteen PBPs in *B. subtilis* and seven of them, PBP1a/b, PBP2a,  
245 PBP2b, PBP2c, PBP3, PBP4 and PBP5, could be identified with Bocillin-FL labeling (Fig. 3B).  
246 The identification of these PBPs is based on a similar labeling experiment with null mutants of the  
247 corresponding genes with the exception of PBP2b (Fig. S3) and their known migration in SDS-  
248 PAGE as determined in a previous study by another group (Popham and Setlow, 1996). The level  
249 of PBP2c encoded by the *pbpF* gene was clearly lower than the levels of the other PBPs. It was

250 detected as a very weak band below the band of PBP2b (Fig. 3B and Fig S3). The two forms of  
251 PBP1, a and b (Popham and Setlow, 1995), could not be separated in the mini-gels used in this  
252 analysis. The data demonstrate that four out of seven PBPs were affected by the PrsA depletion  
253 (Fig. 3B). The levels of active PBP2a, PBP2b, PBP3 and PBP4 were clearly lower in cells  
254 “lacking” PrsA as compared to non-depleted cells, suggesting that their stability is dependent on the  
255 PrsA foldase, whereas the levels of PBP1a/b, PBP2c and PBP5 were not decreased, suggesting their  
256 independence of PrsA. These results are consistent with the similar effects of the PrsA depletion on  
257 GFP-PBP2a and GFP-PBP1a/b observed in the above immunoblotting experiments. The levels of  
258 the four PrsA-dependent PBPs were decreased in a similar manner also in the presence of 20 mM  
259 MgCl<sub>2</sub>, suggesting that magnesium does not suppress their instability (Fig. 3B).

260

261 *The prsA gene can be deleted in the presence of a high concentration of magnesium*

262

263 The suppression of the growth defect of PrsA-depleted *B. subtilis* IH7211 cells in the presence of a  
264 high concentration of magnesium suggests that it might be possible to construct a *prsA* null mutant  
265 (gene replacement) on plates supplemented with magnesium. Indeed this was the case (see  
266 Experimental procedures for the mutant construction). The *prsA* null mutant grew on Antibiotic  
267 Medium 3 –plates supplemented with 20 mM MgCl<sub>2</sub> forming very tiny homogeneous colonies.  
268 Microscopic inspection of cells in the colonies showed that all bacteria were strongly deformed:  
269 either giant vesicular cells or thick twisted rods. These cells looked quite similar as PrsA-depleted  
270 cells of IH7211. In corresponding liquid cultures, the large deformed cells changed so that in  
271 overnight grown cultures small motile cocci-like cells, short bent rods, which were thinner than  
272 those in the exponential growth phase, and also fairly normal-looking rods were observed (see Fig.  
273 4). The appearance of viable cocci-like *prsA* null mutant cells corroborates the evidence about the  
274 involvement of PrsA in lateral cell wall biosynthesis and cell elongation. However, the presence of

275 some rod-shaped bacteria in overnight cultures suggests that they were capable of synthesizing the  
276 cylindrical lateral wall in the absence of PrsA. We did not see on plates any fast-growing  
277 suppressors that would have overgrown the more slowly-growing  $\Delta prsA$  mutant.

278

279 Bocillin-FL labeling of *prsA* null mutant membranes showed that the level of activity of the same  
280 set of PBPs as in the case of PrsA-depleted IH7211 (PBP2a, PBP2b, PBP3 and PBP4) was  
281 decreased (Fig. 3C). Again, no effect was seen on PBP1a/b and PBP5. There was some  
282 experimental variation in the staining of PBP3 in membranes from PrsA-expressing strains  
283 (compare Fig. 3B and 3C), but not with the other PBPs. It may be more unstable than the other  
284 ones. We also determined protein levels of PBP2a and MreC in the null mutant and the wild-type  
285 parental strain by immunoblotting with anti-PBP2a and anti-MreC antibodies, respectively. The  
286 PBP2a amount was clearly lower (>50% reduction) in the absence of PrsA (Fig. 3C), whereas like  
287 in the case of PrsA-depleted IH7211 no effect of PrsA was seen on the MreC amount. This result  
288 suggests that in the absence of PrsA significant misfolding and degradation of several PBPs occurs.  
289 PrsA may not be involved in the folding of MreC.

290

291 *The CssRS two-component system is involved in the quality control of penicillin-binding proteins*

292

293 There are several “periplasmic” proteases which could be involved in the quality control and  
294 degradation of PBPs including HtrA, HtrB, PrsW and WprA (Margot and Karamata, 1996,  
295 Stephenson and Harwood, 1998, Hyyryläinen *et al.*, 2001, Ellermeier and Losick, 2006, Heinrich *et*  
296 *al.*, 2008). Accumulation of misfolded proteins in the cell wall (misfolding or secretion stress)  
297 induces *htrA* and *htrB* gene expression in a manner dependent on the CssRS two-component system  
298 (Hyyryläinen *et al.*, 2001, Darmon *et al.*, 2002) (Hyyryläinen *et al.*, 2005). CssRS is most probably  
299 dedicated to regulate the expression of only these two quality control protease genes (Hyyryläinen

300 *et al.*, 2005). We used a knockout mutation of the *cssS* gene (*cssS::spec*) to study whether CssRS  
301 and the HtrA/B proteases it specifically regulates are involved in PBP degradation. We constructed  
302 strains which express PBP2a-Myc or PBP5-Myc proteins (PBPs modified with a C-terminal Myc-  
303 tag) and determined their levels in the presence and absence of *cssS::spec* and in PrsA-depleted and  
304 non-depleted cells by immunoblotting with anti-Myc antibodies. Bocillin-FL staining was also used  
305 to determine levels of active correctly-folded PBPs in the *cssS::spec* mutant cells.

306

307 Immunoblotting revealed that the *cssS::spec* mutation decreased PBP2a-Myc degradation in PrsA-  
308 depleted cells (Fig. 3D), suggesting that HtrA and HtrB proteases are involved in the degradation of  
309 misfolded PBP2a. The amount of PBP5-Myc as determined by immunoblotting was not  
310 significantly affected by *cssS::spec* (Fig. 3E). It was independent of CssRS and PrsA. However,  
311 Bocillin-FL labeling revealed that in the absence of CssS the level of active PBP5-Myc was clearly  
312 lower in PrsA-depleted cells than in non-depleted cells (Fig. 3E). The PrsA depletion and *cssS::spec*  
313 mutation alone had no effect on the level of active PBP5-Myc. These results show that CssRS,  
314 probably via HtrA/B proteases, and PrsA both are involved in the formation (folding) of active  
315 PBP5 (an overlapping function). The Bocillin-FL labeling (Fig. 3E) also suggested that absence of  
316 CssS (and HtrA/B proteases) increased the level of active PBP2a, PBP2b and PBP4 in PrsA-  
317 depleted cells. It seems that if PBP2a degradation is prevented (*cssS::spec*), at least some active  
318 correctly-folded PBP2a is nevertheless formed with time despite of the absence or very low level of  
319 PrsA. PBP2a and PBP5 are quite different in this respect.

320

321 *Incorrectly-folded PBP2a is formed in PrsA-depleted cells*

322

323 In order to demonstrate that PrsA-depletion causes misfolding of PBP2a, we quantitated the levels  
324 of PBP2a-Myc in membranes of PrsA-depleted and non-depleted cells of *B. subtilis* IH9016 (*Pspac-*

325 *prsA pbpA-myc cssS::spec*) by immunoblotting with anti-Myc antibodies and the proportion of  
326 correctly-folded PBP2a-Myc by Bocillin-FL labeling (Zhao *et al.*, 1999). Similar quantitation was  
327 also performed with the strain *B. subtilis* IH8266 (*Pspac-prsA cssS::spec*) and anti-PBP2a  
328 antibodies. IH8266 expresses wild-type PBP2a instead of PBP2a-Myc.

329

330 The quantitation was performed with a series of two-fold diluted membrane samples analyzed by  
331 SDS-PAGE (Fig. S4). It was observed that the level of Bocillin-FL-binding, correctly-folded full-  
332 length PBP2a-Myc and PBP2a were decreased by 27-40% in PrsA-depleted cells as compared to  
333 non-depleted cells. This indicates that PBP2a misfolding occurs in the absence of PrsA.

334

335 *Peptidoglycan crosslinkage degree is decreased and amount of muropeptides with pentapeptide*  
336 *chain is increased in cells depleted of PrsA*

337

338 To elaborate the cell wall defect caused by the PrsA depletion, we performed a muropeptide  
339 analysis of cell walls isolated from PrsA-depleted and non-depleted cells of IH7211 (*Pspac-prsA*)  
340 and the wild-type strain RH2111. Peptidoglycan was extracted from the cells in the late stationary  
341 phase as described in Experimental procedures and reduced muropeptides were analyzed by RP-  
342 HPLC. The muropeptide profile consisted of 37 peaks, which were analyzed by MALDI-TOF mass  
343 spectrometry (Table 1).

344

345 At a low level of PrsA (*Pspac-prsA* induced with 8  $\mu$ M IPTG) the amount of muropeptides with  
346 pentapeptide chain was significantly increased ( $p < 0.0001$ ) as compared to that in RH2111 with the  
347 wild-type level of PrsA (Table 2). The induction of *Pspac-prsA* expression in IH7211 with 1 mM  
348 IPTG restored a value close to that of the wild-type strain. The PrsA level obtained with the  
349 induction is about 60% of the wild-type PrsA level (Vitikainen *et al.*, 2001). The crosslinkage

350 degree was significantly decreased ( $p < 0.05$ ) by 2 % in the PrsA-depleted cells compared to the  
351 wild-type strain (Table 2) and was restored to the wild-type level by the induction of *Pspac-prsA*  
352 with 1 mM IPTG. Thus, we conclude that the observed differences for peptidoglycan structure are  
353 caused by the PrsA depletion.

354

355 *Van-FL imaging of the cell wall defect of prsA mutants*

356

357 The cell wall defect was further characterized by imaging peptidoglycan biosynthesis in the *prsA*  
358 null mutant and PrsA-depleted cells of *B. subtilis* IH7211 with a fluorescent vancomycin (Van-FL).  
359 Van-FL binds to the terminal D-Ala-D-Ala moieties in non-cross-linked peptidoglycan precursors  
360 and growing glycan chains (Daniel and Errington, 2003, Tiyanont *et al.*, 2006). It has been shown  
361 by using Van-FL staining and fluorescence microscopy that lateral wall peptidoglycan polymers are  
362 synthesized in distinct spots organized in a spiral pattern (Daniel and Errington, 2003, Tiyanont *et*  
363 *al.*, 2006). PBPs that are located in the lateral wall in a similar spiral organization pattern are  
364 responsible for the synthesis of the lateral wall peptidoglycan. On the other hand, PBPs that  
365 normally synthesize the division septum are also capable of synthesizing lateral wall peptidoglycan  
366 (Daniel and Errington, 2003).

367

368 In cells of *B. subtilis* 168 and IH7211 (*Pspac-prsA*) induced with 1 mM IPTG, fluorescence was  
369 mainly seen in the division septum (Fig 4D and 5C, right panels, respectively), but the spiral  
370 synthesis pattern of lateral wall peptidoglycan was also observed particularly in the case of  
371 exponential-phase cells of *B. subtilis* 168 (Fig. 4D). The *prsA* null mutant and PrsA-depleted cells  
372 of IH7211 (8  $\mu$ M and 16  $\mu$ M IPTG) were more intensively fluorescent than wild-type and non-  
373 depleted cells. In thick rods and spherical severely PrsA-depleted cells, fluorescence was strongly  
374 increased in the entire wall. As compared to the fairly moderate effect of severe PrsA depletion on

375 the crosslinkage index, only 2%, the strong diffuse Van-FL fluorescence is surprising. This result  
376 may suggest that peptidoglycan (lipid II) precursors are more abundant in the membrane of PrsA-  
377 depleted than non-depleted cells and distributed evenly around whole deformed cells. Stationary-  
378 phase cells of the *prsA* null mutant, including the small cocci-like ones (Fig. 4B and C), were less  
379 fluorescent than the deformed exponential-phase cells.

380

381 *PrsA-dependent membrane proteins as revealed by membrane proteome analysis*

382

383 The instability of several penicillin-binding proteins in the absence of PrsA suggests that PrsA  
384 facilitates the folding of membrane proteins which have a large “periplasmic” hydrophilic  
385 domain(s). In order to identify the PrsA-dependent membrane proteins, membrane proteome  
386 analysis of IH7211 (*Pspac-prsA*) was performed by using metabolic labeling of PrsA-depleted and  
387 non-depleted cells with  $^{14}\text{N}/^{15}\text{N}$  and mass spectrometric quantification of the changes in relative  
388 amounts of peptides derived from the labeled proteins (see Experimental procedures for  
389 methodological details). The proteome analysis consisted of two biological replicates (M1 and  
390 M2a) and a technical replicate of the experiment M2a (M2b). With the minimum criterion of two  
391 identified peptides, 192 different proteins could be quantified which were predicted to contain  
392 transmembrane helices or signal peptides. A majority of them were predicted to be membrane-  
393 localized proteins (157-171, depending on the algorithm used), either integral membrane proteins or  
394 lipoproteins, but also some established or likely exported/cell wall-associated proteins were  
395 identified (the proteins and their predicted subcellular localizations are listed in Table S1).

396

397 In PrsA-depleted cells, i.e. *Pspac-prsA* induced with 2  $\mu\text{M}$  IPTG, the level of PrsA protein was  
398 about 10% of that in non-depleted cells, i.e. *Pspac-prsA* induced with 1 mM IPTG (Table 3). The  
399 levels of PBP2b, PBP3 and PBP4 were decreased (log2 ratio <-1) in PrsA-depleted cell membranes

400 (Table 3), consistent with the Bocillin-FL labeling and immunoblotting results above. Their amount  
401 was 30-40% of that in non-depleted cells and the decrease was observed in the both biological  
402 replicates as well as in the technical replicate. Furthermore, the level of PBP2a was decreased in  
403 M2a (Table 3). Peptides derived from PBP1a/b, PBP2c, PBP5 and PbpX were also quantified, but  
404 their levels were not significantly changed by PrsA depletion. Only a few other proteins were  
405 quantified decreased, most notably the bacteriophage SPP1 adsorption protein YueB, which was  
406 strongly decreased in all three replicates, being at the lowest only 15% of the level of the PrsA-  
407 expressing cells in M2a (Table 3). Transmembrane topology prediction of YueB (TMHMM)  
408 suggests that it has membrane-spanning segments close to the N- and C-termini and between them a  
409 large “periplasmic” domain (about 900 amino acids). The reduced amount of YueB protein at a low  
410 level of PrsA suggests that this domain folds in a PrsA-dependent manner. The levels of OxaA2,  
411 ComE and YvrA proteins were slightly decreased in one or two of the replicates. The proteome  
412 analysis also suggested that some proteins were more abundant in PrsA-depleted membranes than in  
413 non-depleted ones. Among them are the WapA wall-associated protein and the LytA membrane  
414 protein, which were detected at about two-fold higher levels in two of the replicates (Table S1).

415

416 *PrsA is localized in spots with a spiral-like pattern of organization along the cell membrane*

417

418 In order to find out whether the PrsA lipoprotein is distributed evenly around the cell membrane or  
419 in an uneven manner like MreC and several PBPs, we constructed the *B. subtilis* IH8478 strain  
420 which expresses PrsA modified with a C-terminal Myc-tag. This strain was subjected to a procedure  
421 (see Experimental procedures) in which PrsA-Myc was stained with anti-c-Myc antibodies,  
422 secondary antibodies conjugated with biotin and ExtrAvidin conjugated with Cy3. The stained  
423 PrsA-Myc was visualized by fluorescence microscopy. The localization pattern of PrsA-Myc was  
424 determined both in cells from the exponential and stationary phase of growth. To show specific

425 binding of the antibodies, *B. subtilis* strain 168 (RH2111) was used simultaneously as a negative  
426 control. Indeed, no Cy3 signal was detected in the control strain (see Fig. S5).

427

428 The fluorescence images showed that PrsA is not distributed evenly in the membrane but it is  
429 localized in distinct spots that are lined up in spirals (Fig. 6). This pattern is stable throughout  
430 vegetative growth until stationary phase. However, the spiral structures are better resolved in  
431 exponentially growing cells than in stationary phase cells.

432

433 *PrsA is an oligomeric protein*

434

435 It has been shown that MreC is a dimeric protein and this structure may be important for its putative  
436 function as a scaffold for recruiting PBPs and spatially organizing the lateral cell wall synthesis  
437 (van den Ent *et al.*, 2006). We used formaldehyde cross-linking of PrsA and PrsA-Myc in whole  
438 cells and immunoblotting with anti-c-Myc and anti-PrsA antibodies to study whether PrsA is a  
439 monomeric or dimeric/multimeric protein. The non-random localization pattern suggests that PrsA  
440 may be associated with some other protein(s) which has the same or similar localization pattern, e.g.  
441 MreC or some of the PBPs. The cross-linking approach might also reveal such interactions.

442

443 The cross-linking of cells expressing either wild-type PrsA or PrsA-Myc revealed, in addition to the  
444 33 kDa PrsA or PrsA-Myc monomers, two other PrsA-containing bands of higher molecular  
445 weights, one migrating (in SDS-PAGE) at approximately 65 kDa and the other one slightly above it  
446 (~68 kDa) (Fig. 7). The 65 kDa form was very heat resistant; it did not disappear at heating for 30  
447 minutes at 95°C and analysis in SDS-PAGE in the presence or absence of dithiothreitol (Fig. 7 and  
448 data not shown). A small amount of this protein could also be detected in non-cross-linked cells.  
449 The molecular weight suggests that it might be a PrsA dimer. Consistently, *B. subtilis* PrsA

450 expressed in and purified from *E. coli* contained this same form and its amount increased by cross-  
451 linking of the purified PrsA. The 68 kDa band was detected only in lanes containing cross-linked *B.*  
452 *subtilis* cell or PrsA protein (from *E. coli*) samples and it disappeared by heating at 95°C. It most  
453 probably contains oligomeric PrsA which migrated clearly faster than what is expected for PrsA  
454 trimers or tetramers. A few very weak bands of high-molecular-weight complexes (>68 kDa) were  
455 also detected, but further studies are needed to elucidate whether they contain PrsA associated with  
456 some other components of the membrane/wall.

457

458 Small-angle X-ray scattering (SAXS) was another method to elucidate the multimeric structure of  
459 PrsA (Rodgers *et al.*, 1996). *E. coli*-produced PrsA protein was subjected to SAXS and the radius of  
460 gyration ( $R_g$ ) was determined. PrsA had the  $R_g$  of 27-29 Å (Fig. S6), which further suggests that  
461 PrsA forms oligomers.

462

463

464 **DISCUSSION**

465

466 PrsA peptidyl-prolyl *cis-trans* isomerase has an essential role in extracytoplasmic protein folding in  
467 rod-shaped bacteria. The localization of the enzyme domain at the membrane-cell wall interface  
468 suggests that PrsA may assist the folding of membrane proteins which have large functional  
469 domains on the outer surface of the membrane. In this study we used several methodological  
470 approaches to identify membrane proteins which are dependent on PrsA for folding with the  
471 emphasis on identifying the PrsA-dependent component(s) that is (are) involved in cell shape  
472 determination and/or cell wall synthesis.

473

474 PrsA is most probably involved in lateral cell wall biosynthesis of *B. subtilis* as suggested by the  
475 morphological changes in the absence of PrsA. Severely PrsA-depleted cells are spherical in shape  
476 and pearl necklace-like round-cell chains are formed, but a high concentration of magnesium  
477 probably stabilizes peptidoglycan enabling the bacterium to maintain its rod shape (thick) at very  
478 low PrsA levels. Consistently also small cocci-like cells were formed in stationary phase cultures of  
479 the *prsA* null mutant. In the wild type-like rods of the *prsA* null mutant, the lateral wall synthesis  
480 may have been restored by some compensation mechanism for instance a secondary suppressor  
481 mutation.

482

483 Our results suggest that PrsA is required for lateral cell wall biosynthesis since the folding and  
484 stability of those PBPs which are involved in the lateral wall synthesis are dependent on PrsA.  
485 Levels of several high-molecular-weight penicillin-binding proteins (PBP2a, PBP2b, PBP3 and  
486 PBP4) were significantly decreased in PrsA-depleted cells, in contrast to some other proteins (MreC  
487 and PBP1a/b) located in the same compartment. We could also demonstrate that misfolding of  
488 PBP2a occurred in the absence of PrsA and the misfolded PBP2a was degraded in a manner

489 dependent on the C<sub>ss</sub>RS two-component system. It seems that PrsA is required either directly or  
490 indirectly for PBP2a folding, and most probably also for the folding of the other PrsA-dependent  
491 PBPs, and the primary reason for the growth inhibition and cell wall synthesis defect is probably  
492 insufficient amount of active PBPs. Most likely HtrA and HtrB proteases are involved in the  
493 degradation of misfolded PBP2a, since C<sub>ss</sub>RS is a dedicated regulator of their expression  
494 (Hyyrylainen *et al.*, 2005). HtrA/DegP-type proteases have in addition to the proteolytic activity a  
495 chaperone activity which catalyzes protein folding (Spiess *et al.*, 1999, Antelmann *et al.*, 2003) and  
496 this may explain the effect of C<sub>ss</sub>RS on the folding of PBP5. Our results suggest that PrsA and  
497 C<sub>ss</sub>RS have an overlapping and redundant role in the folding of PBP5, but further work is needed to  
498 characterize the interplay of these components at the molecular level in detail.

499

500 Severe PrsA depletion decreased the crosslinkage degree but only by 2%. This is surprising since  
501 cells are spherical or large rods in severely PrsA-depleted cultures. PBPs that normally synthesize  
502 the division septum, particularly PBP1a/b, which was stable in PrsA-depleted cells, may have taken  
503 a larger role in the crosslinkage/synthesis of the whole cell wall peptidoglycan. This would explain  
504 the relatively moderate decrease in the crosslinkage index. The peptidoglycan structure is only  
505 moderately impaired, but the bacterium is spherical in shape. In contrast to wild-type cells, Van-FL  
506 stained strongly  $\Delta prsA$  and PrsA-depleted exponential-phase cells and the fluorescence was fairly  
507 uniformly distributed around the whole cell membrane. The increased number of remaining  
508 pentapeptide side chains and their even distribution in the wall might explain the increased Van-FL  
509 staining. However, the fairly moderate effect of PrsA-depletion on the peptidoglycan structure may  
510 not be consistent with this explanation. An alternative hypothesis might be that the level of  
511 membrane-bound peptidoglycan precursors was increased in these deformed cells and that the  
512 precursors either moved freely in the membrane or were translocated uniformly across the  
513 membrane.

514

515 Does PrsA assist directly PBP folding or is the effect indirect i.e. via catalysis of folding of a third  
516 component which influences PBP folding? We tried to demonstrate *in vitro* with purified PBP2a  
517 and PrsA a direct role for PrsA in the catalysis of PBP2a folding by measuring the folding kinetics  
518 of denatured PBP2a with the binding of Bocillin-FL, but it did not succeed. The result was very  
519 similar as previously with AmyQ  $\alpha$ -amylase: the denatured protein folded rapidly to correct  
520 enzymatically-active conformation and independently of PrsA. In the compartment at the  
521 membrane-wall interface (“periplasm”), AmyQ folding is strongly dependent on PrsA, but in  
522 protoplasts in the absence of the wall AmyQ folds independently of PrsA (Hyyryläinen *et al.*, 2001,  
523 Vitikainen *et al.*, 2001, Wahlstrom *et al.*, 2003). Thus, the folding assistance requirement is  
524 dependent on the cell wall environment. The situation with PBP2a and other PrsA-dependent PBPs  
525 is probably very similar. PrsA assistance is needed for folding in the “periplasm” only. PBPs, and  
526 also AmyQ, are fairly large proteins and have numerous proline residues. Therefore, it is likely that  
527 direct assistance of chaperones and foldases is needed for their folding in the cell wall environment.  
528 Why is then PBP1a/b independent of PrsA? It is a larger protein than the other PBPs and AmyQ.  
529 One explanation could be that in addition to PrsA and CssRS (HtrA/B), which both are involved in  
530 PBP5 folding, a third chaperone catalyzes PBP1a/b folding.

531

532 A wider search for PrsA-dependent proteins was performed by analyzing PrsA-dependent changes  
533 in membrane proteome by mass-spectrometry. The proteome analysis suggested that PBP2a,  
534 PBP2b, PBP3 and PBP4 are the main PrsA-dependent proteins in the membrane. In addition to  
535 them, only a few other membrane proteins exhibited decreased stability in PrsA-depleted cells, most  
536 significantly the SSP1 receptor YueB. This fairly small set of PrsA-dependent proteins supports a  
537 direct rather than an indirect effect of PrsA on PBP folding. One can envision an indirect effect if  
538 PrsA determines the isomeric state of a prolyl bond in a third component e.g. MreC, the stability of

539 both these conformers is similar and the position of the prolyl switch affects the folding and  
540 stability of PBPs.

541

542 Despite of the rod cell shape, *Corynebacteria* such as *Corynebacterium glutamicum* and  
543 *Corynebacterium diphtheriae*, which belong to the Actinobacteria group of gram-positive bacteria,  
544 do not possess PrsA (Kalinowski *et al.*, 2003). Obviously they do not need a PrsA-like  
545 foldase/chaperone to synthesize the lateral wall and maintain the rod cell shape. The PrsA-  
546 independency may be due to the different mode of lateral wall synthesis in these bacteria as  
547 compared to *B. subtilis* and most probably other rod-shaped Firmicutes; it has been shown that in  
548 *Corynebacterium glutamicum* peptidoglycan is incorporated into the wall via cell poles in a manner  
549 dependent on the DivIVA protein (Daniel and Errington, 2003, Letek *et al.*, 2008). PrsA is also a  
550 dispensable protein in cocci (Drouault *et al.*, 2002, Ma *et al.*, 2006). Since in cocci peptidoglycan is  
551 assembled at the division septum and the hemispherical poles derived from it (Pinho and Errington,  
552 2003), the same reason may explain why PrsA is dispensable in them.

553

554 In *B. subtilis*, the DivIB, DivIC and FtsL cell division proteins and the penicillin-binding protein 2b  
555 form a protein complex that assembles in an interdependent manner (Daniel *et al.*, 2006). It has also  
556 been shown that FtsL and DivIC are unstable in cells depleted of PBP2b (Daniel *et al.*, 2006). FtsL  
557 is a particularly unstable protein in the absence of the interacting proteins (Bramkamp *et al.*, 2006).  
558 PBP2b was one of those PBPs which were degraded in the absence of PrsA and this could affect the  
559 stability of the whole complex. Therefore, we studied the effect of PrsA depletion on the stability of  
560 the divisome proteins by using N-terminal GFP fusions of these proteins. Surprisingly, their  
561 stability was independent of the expression of PrsA in this assay. The membrane proteome analysis  
562 of PrsA-depleted cells also showed a clear decrease in the level of PBP2b but no effect on the level  
563 of DivIB; FtsL and DivIC could not be detected. An NMR study has shown that the DivIB protein

564 of *Geobacillus stearothermophilus* is in two distinctly different conformations depending on the  
565 *cis-trans* isomerization of a Tyr-Pro peptide bond in the extracytoplasmic  $\beta$ -domain and it was  
566 speculated that the *cis-trans* isomerization may modulate the assembly of the divisome complex  
567 (Robson and King, 2006). Our finding that PrsA depletion has no effect on the stability of DivIB,  
568 DivIC and FtsL does not support the hypothesis about a regulatory role of *cis-trans* isomerization in  
569 the divisome complex assembly in *B. subtilis*.

570

571 We also determined the localization of PrsA in the membrane by taking advantage of a *Bacillus*  
572 *subtilis* strain that expresses Myc-tagged PrsA. Since the *prsA-myc* fusion gene is present as a single  
573 copy in the chromosome and under the control of the native *prsA* promoter, artifacts due to  
574 overproduction were avoided. The results showed that PrsA is not randomly distributed in the  
575 membrane. It (PrsA-Myc) was localized to the lateral cell membrane in which it formed distinct  
576 spots organized in a helical pattern. To our knowledge this is the first lipoprotein which has been  
577 shown to have the helical organization pattern. Still little is known about the mechanism underlying  
578 helical distribution of proteins along the membrane. The helical organization of PrsA raises the  
579 question whether it is associated with any of the other proteins with the similar organization pattern  
580 including the cytoskeleton proteins and PBPs. The helical pattern might be dependent on them. It  
581 has been shown that a cytoskeleton protein (MreBH) can determine the helical organization of a  
582 protein (LytE) on the extacytoplasmic side of the membrane (Carballido-Lopez *et al.*, 2006). We  
583 also demonstrated that PrsA forms dimers/oligomers, but the functional significance of the  
584 dimeric/oligomeric structure is still unclear.

585

586 PrsA foldase/chaperone catalyzes post-translocation folding of exported proteins (Jacobs *et al.*,  
587 1993, Hyyryläinen *et al.*, 2001, Vitikainen *et al.*, 2004). It has been shown that overexpression of  
588 PrsA over the wild-type level enhances secretion of some extracellular proteins particularly  $\alpha$ -

589 amylases of *Bacillus* sp. from industrial gram-positive bacteria (Kontinen and Sarvas, 1993,  
590 Vitikainen *et al.*, 2001, Williams *et al.*, 2003, Vitikainen *et al.*, 2005, Lindholm *et al.*, 2006).  
591 Therefore, PrsA is an important tool for increasing yields in industrial protein production especially  
592 thermoresistant  $\alpha$ -amylases for various applications needing degradation of starch to smaller sugars,  
593 including bioethanol production. Now we have shown that PrsA also has a housekeeping role in the  
594 cell. It is required directly or indirectly for PBP folding and lateral cell wall biosynthesis. A class of  
595 most important current antibiotics,  $\beta$ -lactams, exerts the antimicrobial effect by inhibiting PBPs.  
596 Our results suggest that inhibiting PrsA might be an alternative and additive way to inhibit cell wall  
597 biosynthesis of pathogenic rod-shaped bacteria and treat infectious diseases. PrsA targeted  
598 antimicrobials could also inhibit bacterial pathogenesis by inhibiting secretion of critical virulence  
599 factors for instance listeriolysin O and broad-range phospholipase C in *L. monocytogenes* (Alonzo  
600 *et al.*, 2009, Zemansky *et al.*, 2009). Since human and other eukaryotic cells also have functionally  
601 important parvulin-type PPIases, PrsA inhibitors should be PrsA specific. The designing of PrsA  
602 inhibitors could take advantage of structural and mechanistic differences between bacterial and  
603 eukaryotic parvulins (Heikkinen *et al.*, 2009). We can envision that such PrsA inhibitors could  
604 either inhibit specifically the PPIase activity or interfere with functions of the N- or C-terminal  
605 domains, which may be chaperone or interaction domains. Alternatively, eukaryotic cell membrane  
606 could be impermeable to PrsA inhibitors.

607

608

609 **Experimental procedures**

610

611 *Bacterial strains, plasmids and growth conditions*

612

613 *Bacillus subtilis* strains and plasmids used in this study are listed in Table 4 and Table S2,  
614 respectively. *E. coli* DH5 $\alpha$  was used for cloning. Bacteria were grown in LB or TY medium and on  
615 corresponding agar plates at 37°C, but also some other culture media were used for particular  
616 experiments. The metabolic labeling for membrane proteome analysis was performed with cells  
617 grown in a synthetic minimal medium (BMM) (Stulke *et al.*, 1993). Cultivations were performed in  
618 Antibiotic Medium 3 when the effect of magnesium on PrsA-depleted cells and Van-FL staining of  
619 peptidoglycan synthesis in *prsA* null mutant were studied. The growth media were supplemented  
620 with appropriate antibiotics when needed to maintain plasmids and chromosomal plasmid integrants  
621 in the cells. The antibiotics (and their concentrations) used in the cultivations were ampicillin (100  
622  $\mu\text{g/ml}$ ), erythromycin (0.5, 1 or 100  $\mu\text{g/ml}$ ), lincomycin (12.5  $\mu\text{g/ml}$ ), chloramphenicol (5  $\mu\text{g/ml}$ )  
623 and spectinomycin (100  $\mu\text{g/ml}$ ). The expression of *Pspac-prsA* was induced with 1 mM (full  
624 induction) or with 0, 2, 8, 16 or 24  $\mu\text{M}$  (PrsA depletion) IPTG. For the PrsA depletion experiments,  
625 bacteria were taken from fresh agar plates, washed several times in LB medium and then used to  
626 inoculate the cultures. The expression from *Pxyl* was induced with 0.5% xylose.

627

628 *Plasmid constructions*

629

630 To construct pKTH3805, a fragment of the coding region of *prsA* (bp 633-938) was PCR-amplified  
631 with the primers *prsA*myc-fw (5'cacaggtaccatggacgaacattcagcaaag) and *prsA*myc-rv  
632 (5'cacacggccgtttagaattgcttgaagatgaagaagtg). The amplified fragment was inserted into the pGEM-

633 T-Easy vector (Promega). The recombinant plasmid was digested with *KpnI* and *EagI*, the released  
634 '*prsA* fragment was ligated with pMUTIN-cMyc (Kaltwasser *et al.*, 2002) cut with the same  
635 restriction enzymes and the ligation mixture was used to transform competent *E. coli* DH5 $\alpha$  cells.  
636 The obtained plasmid carrying the '*prsA* fragment (pKTH3805) was used to transform *B. subtilis*  
637 RH2111 (168). The Campbell-type integration of pKTH3805 into the *prsA* gene resulted in the  
638 formation of *prsA-myc*, which encodes PrsA bearing a C-terminal Myc-tag. The chromosomal  
639 integration of pKTH3805 replaced the wild-type *prsA* with *prsA-myc*. The viability of the resulted  
640 strain *B. subtilis* IH8478 indicates that PrsA-Myc is functional.

641  
642 *B. subtilis* IH9003 expressing *pbpA-myc* was constructed by transforming 168 with plasmid  
643 pKTH3828. This plasmid was constructed by PCR-amplifying a '*pbpA-myc* fragment with the  
644 primers *pbpA-fw* (5' cacaggatccatagcaaatggtggctaccgc) and *pbpA-rv*  
645 (cacagtcgacttacagatcttctcgctgatcagtttctgttcgttatcagaagacgttggttttctgc) and inserting the fragment  
646 between the *BamHI* and *SalI* sites of the pSG4902 plasmid (Scheffers *et al.*, 2004). The Campbell-  
647 type integration of pKTH3828 into the *pbpA* gene resulted in the formation of *pbpA-myc*.

648  
649 *B. subtilis* IH9025 expressing *dacA-myc* was constructed in a similar manner as *B. subtilis* IH9003.  
650 The '*dacA-myc* fragment in pKTH3831 was PCR-amplified with the primers *dacA-fw* (5'  
651 cacagtcgacggaacagctgaacgcaacg) and *dacA-rv* (5'  
652 cacagaattcttacagatcttctcgctgatcagtttctgttcaaccagccggttaccgtatc) and inserted between the *SalI* and  
653 *EcoRI* sites of pSG4902.

654  
655 To construct pKTH3814, a fragment of the *divIB* gene (bp 295-633) was PCR amplified with the  
656 primers *divIB-fw* (5' cacactcgaggtcatgaacccgggtcaagacc) and *divIB-rv*  
657 (5' cacagaattcaggaagcgatttctgatctcc). The amplified fragment was inserted between the *XhoI* and

658 *EcoRI* sites of the pSG4902 plasmid (Scheffers *et al.*, 2004). The resulted pKTH3814 plasmid was  
659 used to transform *B. subtilis* RH2111. pKTH3814, upon integration into the *B. subtilis*  
660 chromosome, disrupted the native *divIB* gene and created a *gfp-divIB* fusion (*B. subtilis* IH8473),  
661 which is expressed from the xylose-inducible *P<sub>xyl</sub>* promoter.

662

663 *B. subtilis* IH8471 expressing *gfp-divIC* was constructed in a similar manner as *B. subtilis* IH8473.  
664 A fragment of the *divIC* gene (bp 455-755) was PCR amplified with the primers *divIC-fw*  
665 (5'cacaggatccctttgaattttccaggaacga) and *divIC-rv* (5'cacactcgaggacgtaatcctcctcctcaattg). The  
666 *divIC* fragment was cloned in the pGEM-T-Easy vector. The fragment was released by digesting  
667 with *Bam*HI and *Xho*I, and inserted into pSG4902. *B. subtilis* RH2111 was transformed with the  
668 obtained plasmid, pKTH3806.

669

#### 670 *Construction of the prsA null mutant*

671

672 Chromosomal DNA was isolated from *B. subtilis* IH7075 (in the culture collection of THL) and  
673 used to transform *B. subtilis* 168 (RH2111). In IH7075, the *prsA* gene is deleted and replaced with  
674 the *cat* gene from pC194. The IH7075 strain also harbors plasmid pKTH3327, which carries *prsA*  
675 under the control of the *Pspac* promoter and complements the chromosomal *prsA* deletion. The  
676  $\Delta$ *prsA* mutation deletes the coding sequence of *prsA*, and 153 bp and 75 bp of the up- and  
677 downstream regions, respectively. The *prsA* null mutants of 168 were selected on Antibiotic  
678 Medium 3 –plates containing 20 mM MgCl<sub>2</sub> and chloramphenicol (5 µg/ml).

679

#### 680 *SDS-PAGE and immunoblot analysis of PrsA, MreC, PBP2a and GFP-fusion proteins*

681

682 Whole cell samples were prepared from cultures in the late exponential (Klett100+1h) or early  
683 stationary (Klett100+3h) phase of growth. Cells were harvested by centrifugation from 1 ml of  
684 culture, resuspended in 50  $\mu$ L of protoplast buffer (20 mM potassium phosphate pH7.5, 15 mM  
685  $MgCl_2$ , 20% sucrose and 1 mg/ml lysozyme) and incubated at 37°C for 20 minutes. Then 50  $\mu$ l of  
686 2xLaemmli sample buffer was added and the samples were boiled for 10 minutes at 100°C. Proteins  
687 were separated in SDS-PAGE and blotted onto a PVDF nylon filter (Immobilon-P transfer  
688 membrane; Millipore). The immunodetection of PrsA, PrsA-Myc, MreC, PBP2a and GFP-fusion  
689 proteins was performed using specific antibodies against these proteins (or Myc-tag) and goat anti-  
690 rabbit IgG (H+L)-HRP conjugate (Bio-Rad). ECL reactions were performed using an Immun-Star  
691 WesternC kit according to the instructions of the manufacturer (Bio-Rad) and proteins were  
692 visualized and quantitated with a FluorChem HD2 imager and AlphaEase FC software  
693 (AlphaInnotech).

694

695 *Isolation of bacterial cell membranes and Bocillin-FL labeling of penicillin-binding proteins*

696

697 Bacterial cell membranes were prepared from 500 ml of culture in LB medium. Cells were  
698 harvested at the cell density of Klett100 by centrifugation, washed once with potassium phosphate  
699 buffer (20 mM potassium phosphate pH 7.5, 140 mM NaCl) and resuspended in the washing buffer.  
700 The cells were disrupted by passing the suspension through a French press cell twice at 20,000  
701 lb/in<sup>2</sup>. The cell lysate was centrifuged at 8000g for 10 minutes, followed by centrifugation of the  
702 supernatant at 217,500g for 1h. The membrane pellet was resuspended in the phosphate buffer (1  
703 ml). Protein concentrations of the membrane preparations were determined using a 2-D Quant Kit  
704 (GE Healthcare) or Micro BCA (Pierce) according to the instructions of the manufacturers.

705

706 In the Bocillin-FL labeling reaction, cell membranes (300 µg protein) were treated with 10 µM  
707 Bocillin-FL in a final volume of 100 µl. The reaction mixtures were incubated at 35°C for 30  
708 minutes, followed by addition of 100 µl 2×Laemmli buffer and incubation at 100 °C for 3 minutes.  
709 Samples corresponding 15 µg of protein were separated in 10% SDS-PAGE. Fluorescent PBPs  
710 were visualized using a fluoroimager Typhoon 9400 (Amersham Biosciences) with excitation at  
711 488 nm and emission at 520 nm. Levels of active Bocillin-FL-labeled PBP2a were quantitated with  
712 the ImageQuantTL software (Amersham Biosciences).

713

#### 714 *Peptidoglycan extraction and muropeptide analysis*

715

716 *Bacillus subtilis* cells were grown in LB medium, a volume corresponding  $V \times OD = 300$  was taken in  
717 the late stationary phase (Klett100+6h) and the cells were harvested by centrifugation.  
718 Peptidoglycan extraction and muropeptide analysis were performed as described previously for  
719 *Lactococcus lactis* (Courtin *et al.*, 2006). Purified peptidoglycan was digested with mutanolysin  
720 (muramidase from *Streptomyces globisporus*; Sigma-Aldrich). Soluble muropeptides were reduced  
721 with sodium borohydride as described (Atrih *et al.*, 1999) and separated on a Hypersil-100 column  
722 (C18, 250 by 4.6 mm, 5 µm; Thermo Finnigan) at 50°C by RP-HPLC. The column was eluted with  
723 10 mM ammonium phosphate pH 4.6 and 0.18% sodium azide for 5 minutes, followed by a linear  
724 gradient of methanol (0-20%) for 270 min as described previously (Courtin *et al.*, 2006). Samples  
725 of eluted muropeptides were analyzed by MALDI-TOF mass spectrometry (Voyager DE STR,  
726 Applied Biosystems, Framingham, MA) with  $\alpha$ -cyano-4-hydrocinnamic acid matrix. For most  
727 fractions, 1 µl sample was sufficient. For less abundant fractions, 100 µl was concentrated on a ZIP-  
728 Tip C18 pipette tip (Millipore) and eluted with 1 µl of solvent (50% acetonitrile and 0.15%  
729 trifluoroacetic acid) prior to analysis.

730 The crosslinkage degree was calculated according to (Glauner, 1988) with the formula:  $(1/2$   
731  $\Sigma \text{ dimers} + 2/3 \Sigma \text{ trimers} + 3/4 \Sigma \text{ tetramers}) / \Sigma \text{ all muropeptides}$ .

732 The percentage of muropeptides with a certain side peptide chain (X = di, tri, tetra and penta) with  
733 free COOH (donor chain) was calculated according to Glauner (1988).

734 Percentage (X) =

735  $[\Sigma \text{ monomers(X)} + 1/2 \Sigma \text{ dimers(X)} + 1/3 \Sigma \text{ trimers(X)} + 1/4 \Sigma \text{ tetramers(X)}] / \Sigma \text{ all muropeptides}$ .

736 Statistical analysis of the data was performed with Statgraphics Plus software (Manugistics,  
737 Rockville, MD, USA). The results obtained with two strains were compared with a two-sample  
738 comparison analysis and a *t*-test.

739

740 *Van-FL staining and fluorescence microscopy*

741

742 *Bacillus subtilis* strains 168 and  $\Delta prsA$  were grown over night in 10 ml Antibiotic medium 3  
743 (Difco) supplemented with 20 mM MgCl<sub>2</sub> and 5 µg/ml chloramphenicol when needed. Over night  
744 cultures were diluted in 20 ml fresh medium to OD<sub>600</sub>=0.1 and grown 24 hours. Cells were  
745 collected for Van-FL staining at exponential, stationary and late stationary phases. *B. subtilis* strain  
746 IH7211 was grown over night on a TY agar plate supplemented with 1 µg/ml erythromycin.  
747 Material from plate was suspended in phosphate-buffered saline (PBS) to OD<sub>600</sub>=1.0 and washed  
748 three times with 1 ml PBS. 20 µl of the suspension was used to inoculate 10 ml TY containing 1  
749 µg/ml erythromycin and IPTG at three different concentrations: 8 µM, 16 µM and 1 mM. At  
750 OD<sub>600</sub>=0.6, samples were collected for Van-FL staining.

751

752 0.5 ml of a culture was incubated 20 minutes with 1 µg/ml fluorescently-labeled vancomycin  
753 (BODIPY® FL vancomycin, Invitrogen) mixed in 1:1 ratio with unlabeled vancomycin (Sigma).  
754 The cells were spotted on microscope slides (Knittel Gläser, Germany). The Van-FL-stained cells  
755 were viewed immediately under a fluorescence microscope (Olympus IX71) equipped with a Cool

756 Snap HQ2 camera (Photometrics). Van-FL fluorescence was visualized with a bandpass 470/40 nm  
757 excitation filter and a bandpass 525/50 nm emission filter. Images were analyzed using ImageJ  
758 (<http://rsb.info.nih.gov/nih-image/>) and Adobe Photoshop CS2 Version 9.0.

759

#### 760 *Electron microscopy*

761

762 For electron microscopy, cells were fixed with 2.5% glutaraldehyde overnight at 4°C as has been  
763 described (Leaver and Errington, 2005). The fixed cells were washed twice in phosphate buffer and  
764 then treated with 1% osmium tetroxide for 1 hour. The samples were dehydrated with a series of  
765 treatments with ethanol and acetone, followed by embedding in Epon resin. The microscopy was  
766 performed in the Institute of Biotechnology, University of Helsinki, by using a JEOL 1200EX II  
767 electron microscope.

768

#### 769 *Quantitation of the effect of a minimal PrsA concentration on the membrane proteome of B. subtilis*

770

771 For metabolic labeling, *B. subtilis* IH7211 ( $P_{spac}$ -*prsA*) was grown aerobically at 37°C in a synthetic  
772 minimal medium (BMM). The medium was either supplemented with <sup>15</sup>N-ammonium sulfate, <sup>15</sup>N-  
773 L-tryptophan and <sup>15</sup>N-L-glutamate (Cambridge Isotope Laboratories, Andover, USA) or <sup>14</sup>N-  
774 ammonium sulfate, <sup>14</sup>N-L-tryptophan and <sup>14</sup>N-L-glutamate. Cells from overnight cultures grown  
775 with 40 μM IPTG were washed with warm BMM and used to inoculate the cultures for the  
776 metabolic labeling. In order to realize two different biological states, 2 μM IPTG was used in the  
777 cultivation M1 with the light form of nitrogen source and 1 mM IPTG with the heavy one (see  
778 below). A biological replicate (M2a) was performed with identical cultures but the labels were  
779 switched. Cells were harvested in the exponential phase of growth and equivalent OD-units of

780 bacteria either grown with  $^{15}\text{N}$ -BMM or  $^{14}\text{N}$ -BMM were combined in proportion 1:1 and stored at -  
781 20°C.

782

783 The combined cells were disrupted on ice using a French press cell, followed by separation of cell  
784 debris by centrifugation and extraction of cell membranes according to the method described by  
785 Eymann and collaborators (Eymann *et al.*, 2004). Membranes were centrifuged at 100,000g for 60  
786 min at 4°C, followed by purification steps with high salt buffer (20 mM Tris-HCl, pH7.5, 10 mM  
787 EDTA, 1 M NaCl, Complete Protease Inhibitor (Roche)), alkaline  $\text{Na}_2\text{CO}_3$  buffer (100 mM  
788  $\text{Na}_2\text{CO}_3$ -HCl, pH 11, 10 mM EDTA, 100 mM NaCl) and 50 mM TEAB. Finally the purified  
789 membranes were solubilized in SDS-PAGE sample buffer containing 20% SDS. Proteins were  
790 analyzed using GeLC-MSMS analyzing the resulting tryptic digests using an UPLC coupled to an  
791 LTQ-Orbitrap. In addition to the two biological replicates, a technical replicate, M2b, was  
792 performed. For this replicate, the proteins of M2a were separated and analyzed with GeLC-MSMS  
793 for a second time. The data-analysis and relative quantification of the proteins was performed as  
794 described in Supporting Information (Table S1).

795

796 *Determination of the localization of PrsA*

797

798 Single colonies of *B. subtilis* 168 and IH8478 (*prsA-myc*) grown on TY plates were used to  
799 inoculate 5 ml TY liquid medium. Overnight cultures were diluted in 20 ml TY medium to  $\text{OD}_{600} =$   
800 0.1 and grown till stationary phase. TY medium was supplemented with erythromycin to a final  
801 concentration of 1  $\mu\text{g}/\text{ml}$  when needed. Samples for immunofluorescence assay were collected 2  
802 hours before and 4 hours after the transition from the exponential to the stationary growth phase  
803 (Fig. 6). Immunofluorescence staining was performed according to the method described by Harry  
804 and collaborators (Harry *et al.*, 1995) with the modifications described below.

805

806 Cells were fixed and made permeable as follows. 0.5 ml of bacterial culture in TY was mixed with  
807 an equal volume of 2×fixative solution containing 2.68 % paraformaldehyde and 0.0050 %  
808 glutaraldehyde and incubated for 15 min at room temperature (21-23°C) and 30 min on ice. After  
809 fixation the cells were washed three times in phosphate-buffered saline (PBS) and resuspended in  
810 GTE (50 mM glucose, 20 mM Tris-HCl pH 7.5, 10 mM EDTA). A fresh lysozyme solution in GTE  
811 was added to an aliquot of cells to a final concentration of 2 mg/ml and cells were immediately  
812 spotted on multiwell slides (MP Biomedicals LLC) coated with 0.01 % poly-L-lysine (Sigma-  
813 Aldrich). After 5 - min incubation wells were washed with PBS and left to air dry.

814

815 For immunostaining, cells were blocked with PBS containing 2% BSA and 0.01% Tween (hereafter  
816 referred to as “blocking solution”) for 15 min at room temperature. Next cells were incubated with  
817 mouse anti-c-Myc antibodies (Gentaur) diluted 1:1000 in the blocking solution for 1 hour at room  
818 temperature. After washing the cells 10 times with PBS, secondary anti-mouse biotin-conjugated  
819 antibody (Sigma-Aldrich) diluted 1:500 in the blocking solution was added, followed by incubation  
820 in the dark at room temperature for 1 hour. Cells were washed again 10 times with PBS and  
821 incubated 1 hour with 1:25 diluted ExtrAvidin Cy3 conjugate (Sigma-Aldrich) at room temperature  
822 in the dark. Samples were washed 10 times with PBS and mounted with Vectashield mounting  
823 medium (Vector Laboratories). Slides were stored at -20°C.

824

825 Sample imaging was performed using a wide-field Zeiss Axioscop50 fluorescence microscope (Carl  
826 Zeiss, Oberkochen, Germany) equipped with a Princeton Instruments 1300Y digital camera. Cy3  
827 fluorescence was visualized with a bandpass (546 /12 nm) excitation filter, a 560 nm dichromatic  
828 mirror, and a bandpass (575–640 nm) emission filter. Images were analyzed using ImageJ  
829 (<http://rsb.info.nih.gov/nih-image/>) and Adobe Photoshop CS2. Wide-field images were corrected

830 for bleaching and unstable illumination using the Huygens Professional deconvolution software by  
831 Scientific Volume Imaging (<http://www.svi.nl/>).

832

833 *Cross-linking of PrsA*

834

835 Protein cross-linking was performed with 1% formaldehyde as has been described (Jensen *et al.*,  
836 2005). Bacteria were grown in LB medium at 37°C until culture density was 100 Klett units. Cells  
837 were harvested from 1 ml of the culture, washed once with 1 ml 0.1 M sodium phosphate buffer  
838 (pH 6.8) and cross-linked with formaldehyde for 10 minutes at room temperature. Cells were  
839 pelleted, washed once in phosphate buffer and solubilized in SDS-PAGE lysis buffer as has been  
840 described (Healy *et al.*, 1991). Cross-linked PrsA or PrsA-Myc proteins were analyzed by SDS-  
841 PAGE and immunoblotting. Samples were heated either at 37°C for 10 minutes or at 95°C for 30  
842 minutes (breaks formaldehyde cross-links) prior to SDS-PAGE.

843 **Table 1.** Muropeptide structures and quantification from peptidoglycan of *B. subtilis* RH2111 and  
 844 conditional mutant IH7211 (*P<sub>spac</sub>-prsA*) cultured with 8  $\mu$ M or 1 mM IPTG.

845

Peak number <sup>a</sup>	Proposed structures <sup>b,c</sup>	Amount of muropeptides (%) <sup>d</sup>		
		RH2111	IH7211 8 $\mu$ M IPTG	IH7211 1 mM IPTG
1	ds-tri	2.65	1.26	2.63
2	ds-tri (deAc)	0.53	1.00	0.53
3	ds-tri with 1 amidation	10.58	13.39	10.84
4	ds-tri (deAc) with 1 amidation	2.07	1.70	1.70
5	ds-tetra	0.32	0.31	0.22
6	ds-tetra with 1 amidation	0.22	0.33	0.26
7	ds-di	1.39	1.73	1.62
8	ds-tetra with 1 amidation	0.75	1.02	0.71
9	ds-tri-di with 2 amidations	1.06	1.85	1.25
10	ds-tetra with 2 amidations	0.85	0.83	0.82
11	ds-tri-tetra with 2 amidations	0.44	0.22	0.53
12	ds-penta with 1 amidation	0.39	0.95	0.33
13	ds-tri-ds-tetra with 1 amidation and missing GlcNac	1.34	1.19	1.68
14	ds-tri-ds-tetra	1.44	0.80	1.16
15	ds-tetra-tetra with 1 amidation	0.32	0.27	0.28
16	ds-tri-ds-tetra with 1 amidation	8.78	6.63	10.51
17	ds-tri-ds-tetra with 2 amidations and missing GlcNac	0.66	1.43	0.86
18	anhydro ds-tri with 1 amidation	0.10	0.17	1.23
	ds-tri-ds-tetra (deAc) with 1 amidation	2.29	0.86	1.23
19	ds-tri-ds-tetra (deAc) with 1 amidation	1.15	0.69	1.06
20	ds-tri-ds-tetra with 1 amidation	1.89	1.31	2.12
21	ds-tri-ds-tetra with 2 amidations	26.34	30.79	26.32
22	ds-tri-ds-tetra (deAc) with 2 amidations	7.90	6.87	6.04
23	ds-tri-ds-tetra (deAc) with 2 amidations	5.26	4.81	4.37
24	ds-tri-ds-tetra (deAc x 2) with 2 amidations	1.69	1.22	1.15
25	ds-tetra-ds-tetra with 2 amidations	0.87	1.08	0.91
26	ds-penta-ds-tetra with 1 amidation	0.49	0.59	0.38
27	ds-penta-ds-tetra with 2 amidations	1.63	1.95	1.41
28	ds-tetra-ds-tetra with 3 amidations	0.18	0.12	0.19
	ds-tri-ds-tetra-ds-tetra with 3 amidations	0.18	0.12	0.19
29	ds-penta-ds-tetra (deAc) with 2 amidations	0.68	0.83	0.54
30	ds-tri-ds-tetra +Ac with 2 amidations	0.51	0.20	0.59
	ds-tri-ds-tetra-ds-tetra with 2 amidations	0.51	0.20	0.59
31	ds-tri-ds-tetra-ds-tetra with 2 amidations	2.20	1.38	2.95
32	ds-tri-ds-tetra-ds-tetra with 3 amidations	6.01	6.01	6.67
33	ds-tri-ds-tetra-ds-tetra (deAc) with 3 amidations	3.30	2.27	2.77
34	ds-tri-ds-tetra-ds-tetra (deAc x 2) with 3 amidations	1.18	0.66	1.05
35	ds-penta-ds-tetra-ds-tetra with 3 amidations	0.48	0.41	0.46
36	anhydro ds-tri-ds-tetra with 2 amidations	0.78	1.67	0.80
37	anhydro ds-tri-ds-tetra with 2 amidations	0.24	0.38	0.53
	ds-tri-ds-tetra-ds-tetra-ds-tetra with 4 amidations	0.37	0.46	0.53

846

847 <sup>a</sup> Peak numbers refers to the different peaks separated by RP-HPLC from the muropeptide digest of

848 *B. subtilis* peptidoglycan.

849 <sup>b</sup> Proposed structures according to the masses determined by Maldi-Tof and to the identifications by  
850 Atrih et al. (1999).

851 <sup>c</sup> ds, disaccharide (GlcNAc-MurNAc); tri, tripeptide (L-Ala-D-Glu-mDAP); tetra, tetrapeptide (L-  
852 Ala-D-Glu-mDAP-D-Ala); penta, pentapeptide (L-Ala-D-Glu-mDAP-D-Ala-D-Ala)  
853 mDAP, meso-diaminopimelic acid; deAc, deacetylated; +Ac, acetylated.

854 <sup>d</sup> Percentage of each peak was calculated as the ratio of the peak area over the sum of areas of all  
855 the peaks identified in the table. The values presented are the mean values obtained on three  
856 independent experiments for each strain.

For Peer Review

857 **Table 2.** Relative amounts of monomers, dimers, trimers and tetramers and of the different peptide  
 858 side chains with a free carboxyl group (acceptor chain) in the peptidoglycan of the different strains.  
 859

Muropeptides <sup>a</sup>	Amount of muropeptides (%) <sup>b</sup>		
	RH2111	IH7211 8 $\mu$ M IPTG	IH7211 1 mM IPTG
Monomers	19.8	22.7	20.9
Dimers	65.9	65.8	63.9
Trimers	13.9	11.1	14.7
Tetramers	0.4	0.5	0.5
Crosslinkage degree	42.5 (0.9)	40.6 (0.7)	42.1 (0.7)
Dipeptide	1.4 (0.1)	1.7 (0.2)	1.6 (0.2)
Tripeptide	51.4 (0.5)	51.7 (0.4)	51.9 (0.2)
Tetrapeptide	2.8 (0.5)	3.2 (0.1)	2.7 (0.3)
Pentapeptide	2.0 (0.1)	2.8 (0.1)	1.7 (0.1)

860

861 <sup>a</sup> The crosslinkage degree and the relative amounts of the different peptide side chains were  
 862 calculated according to Glauner (Glauner *et al.*, 1988).

863 <sup>b</sup> Percentages presented are the mean values of three independent determinations for each strain  
 864 according to muropeptide structure determination presented in Table 1. Values in brackets are  
 865 standard deviations.

866

867

868

869

**Table 3.** Decreased levels of membrane proteins with a large “periplasmic” domain in PrsA-depleted cells.

Gene names	Protein Names	M1				M2a				M2b			
		WEIGHTED AVERAGE RATIO (given by CENSUS)	Normalized Ratio	LOG 2 RATIO	Number of quantified Peptides	WEIGHTED AVERAGE RATIO (given by CENSUS)	Normalized Ratio	LOG 2 RATIO	Number of quantified Peptides	WEIGHTED AVERAGE RATIO (given by CENSUS)	Normalized Ratio	LOG 2 RATIO	Number of quantified Peptides
<i>prsA</i>	Foldase protein PrsA	0,12	0,12	-3,01	12	0,16	0,13	-2,90	11	0,15	0,12	-3,11	6
<i>pbpB</i>	Penicillin-binding protein 2b	0,32	0,32	-1,64	5	0,41	0,34	-1,55	10	0,39	0,30	-1,73	7
<i>pbpC</i>	Penicillin-binding protein 3	0,40	0,41	-1,30	8	0,41	0,34	-1,55	17	0,41	0,32	-1,66	10
<i>yueB</i>	Bacteriophage SPP1 adsorption protein YueB	0,44	0,44	-1,18	2	0,18	0,15	-2,73	12	0,26	0,20	-2,31	10
<i>pbpD</i>	Penicillin-binding protein 4	0,46	0,47	-1,09	3	0,48	0,40	-1,32	6	0,49	0,38	-1,40	6
<i>comEA</i>	ComE operon protein 1	0,83	0,84	-0,25	3	0,53	0,44	-1,18	2	0,94	0,73	-0,46	2
<i>oxaA2</i>	Membrane protein OxaA 2	1,79	1,81	0,85	2	0,45	0,38	-1,41	4	0,48	0,37	-1,43	4
<i>yvrA</i>	YvrA	0,75	0,76	-0,39	5	0,69	0,58	-0,80	6	0,60	0,46	-1,11	3
<i>pbpA</i>	Penicillin-binding protein 2a					0,41	0,34	-1,55	2	0,75	0,58	-0,78	3

870

871

**Table 4.** *B. subtilis* strains used in this study.

Strain <sup>a</sup>	Relevant genotype	Reference
IH7211	168 <i>prsA</i> ::pKTH3384 <i>Pspac-prsA</i>	(Vitikainen <i>et al.</i> , 2001)
IH8266	168 <i>prsA</i> ::pKTH3384 <i>Pspac-prsA cssS</i> :: <i>spec</i>	This study
IH8435	3417 <i>prsA</i> ::pKTH3384 <i>Pspac-prsA</i>	This study
IH8437	3103 <i>prsA</i> ::pKTH3384 <i>Pspac-prsA</i>	This study
IH8441	2083 <i>prsA</i> ::pKTH3384 <i>Pspac-prsA</i>	This study
IH8445	JAH66 <i>prsA</i> ::pKTH3384 <i>Pspac-prsA</i>	This study
IH8456	168 $\Delta$ <i>pbpF</i> :: <i>ery</i>	This study
IH8458	168 <i>dacA</i> :: <i>cat</i>	This study
IH8460	168 $\Delta$ <i>pbpD</i> :: <i>ery</i>	This study
IH8462	168 $\Delta$ <i>ponA</i> :: <i>spec</i>	This study
IH8464	168 <i>pbpC</i> :: <i>spec</i>	This study
IH8471	168 <i>divIC</i> ::pKTH3806 <i>Pxyl-gfp-divIC</i>	This study
IH8473	168 <i>divIB</i> ::pKTH3814 <i>Pxyl-gfp-divIB</i>	This study
IH8478	168 <i>prsA</i> ::pMUTIN-cMyc <i>prsA-myc</i>	This study
IH8480	IH8471 <i>prsA</i> ::pKTH3384 <i>Pspac-prsA</i>	This study
IH8483	IH8473 <i>prsA</i> ::pKTH3384 <i>Pspac-prsA</i>	This study
IH8999	168 <i>pbpA</i> :: <i>ery</i>	This study
IH9003	168 <i>pbpA</i> ::pKTH3828 <i>pbpA-myc</i>	This study
IH9013	IH9003 <i>cssS</i> :: <i>spec</i>	This study
IH9016	IH9013 <i>prsA</i> ::pKTH3384 <i>Pspac-prsA</i>	This study
IH9024	168 $\Delta$ <i>prsA</i>	This study
IH9025	168 <i>dacA</i> ::pKTH3831 <i>dac-myc</i>	This study
IH9027	IH9003 <i>prsA</i> ::pKTH3384 <i>Pspac-prsA</i>	This study
IH9028	IH9025 <i>prsA</i> ::pKTH3384 <i>Pspac-prsA</i>	This study
IH9029	IH9028 <i>cssS</i> :: <i>spec</i>	This study
2083 (RH2225)	168 <i>ponA</i> ::pSG1492 <i>Pxyl-gfp-ponA</i>	(Scheffers <i>et al.</i> , 2004)
3103 (RH2227)	168 <i>pbpA</i> ::pSG5043 <i>Pxyl-gfp-pbpA</i>	(Scheffers <i>et al.</i> , 2004)
3417 (RH2224)	168 <i>mreC</i> ::pSG5276 <i>Pxyl-gfp-mreC</i>	(Leaver and Errington, 2005)
DPVB207 (RH2223)	PS832 $\Delta$ <i>pbpH</i> :: <i>spec pbpA</i> :: <i>ery amyE</i> :: <i>Pxyl-pbpH</i>	(Wei <i>et al.</i> , 2003)
PS1869 (RH2234)	PS832 $\Delta$ <i>pbpF</i> :: <i>ery</i>	(McPherson <i>et al.</i> , 2001)
PS1900 (RH2235)	PS832 <i>dacA</i> :: <i>cat</i>	(Popham <i>et al.</i> , 1996)
PS2022 (RH2236)	PS832 $\Delta$ <i>pbpD</i> :: <i>ery</i>	(Popham and Setlow, 1996)
PS2062 (RH2237)	PS832 $\Delta$ <i>ponA</i> :: <i>spec</i>	(McPherson <i>et al.</i> , 2001)
PS2328 (RH2238)	PS832 <i>pbpC</i> :: <i>spec</i>	(Wei <i>et al.</i> , 2003)
PS832	wild type, Trp <sup>+</sup> revertant of 168	(Wei <i>et al.</i> , 2003)
168 (RH2111)	<i>trpC2</i>	(Kunst <i>et al.</i> , 1997)
JAH66 (RH2229)	1012 <i>amyE</i> :: <i>gfp-ftsL</i>	(Heinrich <i>et al.</i> , 2008)

a. In parenthesis are shown the strain codes in the collection of THL.

873

874 **Figure legends**

875

876 **Fig. 1.** Morphological changes of PrsA-depleted cells. Electron microscopy of PrsA-depleted cells  
877 was performed as described in Experimental procedures. The scale bars – 2  $\mu$ m.

878 A. IH7211 (*Pspac-prsA*) induced with 8  $\mu$ M IPTG.

879 B. RH2111 wild-type strain.

880 C-D. IH7211 (*Pspac-prsA*) in the absence of IPTG.

881 E. IH7211 (*Pspac-prsA*) in the absence of IPTG and in the presence of 20 mM MgCl<sub>2</sub>.

882 F. IH7211 (*Pspac-prsA*) induced with 1 mM IPTG.

883

884 **Fig. 2.** The suppression of the growth defect of PrsA-depleted cells by 20 mM MgCl<sub>2</sub>. Cells of  
885 IH7211 (*Pspac-prsA*) were grown in Antibiotic Medium 3 with the supplementations indicated.

886

887 **Fig. 3.** PrsA depletion destabilizes penicillin-binding proteins.

888 A. Effect of PrsA depletion on the cellular level of GFP-PBP2a. Whole cell samples from *B. subtilis*  
889 IH8437 (*Pxyl-gfp-pbpA Pspac-prsA*) were prepared as described in Experimental procedures and  
890 levels of GFP-PBP2a and PrsA were determined by immunoblotting and chemiluminescence  
891 detection. *Pxyl* was induced with 0.5% xylose.

892 B. Cytoplasmic membranes were isolated and levels of active PBPs were visualized by staining  
893 with Bocillin-FL (see Experimental procedures) and separation in SDS-PAGE. Effect of PrsA  
894 depletion and magnesium on the levels of active PBPs. The genes encoding PBP1a/b, PBP2a,  
895 PBP2b, PBP2c, PBP3, PBP4 and PBP5 are *ponA*, *pbpA*, *pbpB*, *pbpF*, *pbpC*, *pbpD* and *dacA*,  
896 respectively.

897 C. Effect of the *prsA* null mutation ( $\Delta$ *prsA*; *B. subtilis* IH9024) on levels of active PBPs (Bocillin  
898 FL staining) and total levels of PBP2a, MreC and PrsA (immunoblotting).

899 D. Levels of PBP2a-Myc in PrsA-depleted cells in the presence (*B. subtilis* IH9027; *pbpA-myc*  
900 *Pspac-prsA*) and absence of CssS (*B. subtilis* IH9016; *pbpA-myc Pspac-prsA cssS::spec*) as  
901 determined by immunoblotting.

902 E. Misfolding of PBP5-Myc in the absence of both PrsA and CssS. Bocillin-FL staining of active  
903 PBPs and immunoblotting of total PBP5-Myc in membranes of PrsA-depleted and non-depleted  
904 cells of IH9028 (*dacA-myc Pspac-prsA*) and IH9029 (*dacA-myc Pspac-prsA cssS::spec*).

905

906 **Fig. 4.** Van-FL staining of *B. subtilis*  $\Delta$ *prsA* mutant IH9024 (A-C) and 168 (D). Left panels – phase  
907 contrast images, right panels – Van-FL staining. Scale bar represents 6  $\mu$ m (the same for all the  
908 images).

909 A and D. Exponential growth phase.

910 B. Stationary phase.

911 C. Late stationary phase.

912

913 **Fig. 5.** Van-FL staining of *B. subtilis* strain IH7211 (*Pspac-prsA*). Left panels – phase contrast  
914 images, right panels – Van-FL staining. *Pspac-prsA* expression was induced with IPTG as  
915 indicated. Scale bar represents 6  $\mu$ m (the same for all the images).

916

917 **Fig. 6.** Immunolocalization of PrsA-Myc in *Bacillus subtilis* IH8478 strain in exponential (A – C)  
918 and stationary phase (D – F). Immunostaining has been described in Experimental procedures.  
919 Scale bar – 2  $\mu$ m. The upper panel shows growth curves of *B. subtilis* IH8478 and *B. subtilis* 168,  
920 the parental strain which does not express PrsA-Myc. Arrows indicate time points when samples  
921 were collected for immunofluorescence microscopy.

922 A and D. Phase contrast pictures.

923 B and E. Fluorescence pictures of Cy3-stained cells.

924 C and F, Fluorescence pictures after deconvolution.

925

926 **Fig. 7.** PrsA dimers and oligomers as revealed by formaldehyde cross-linking of whole *B. subtilis*  
927 cells and purified PrsA. Cross-linked PrsA (A) or PrsA-Myc (B) complexes were detected by  
928 immunoblotting.

929 A. Non-lipomodified PrsA expressed in the cytoplasm of *E. coli* and purified (lanes 1-3) and  
930 lipomodified PrsA in whole cells of *B. subtilis* RH2111 (lanes 4-7). Heating of non-cross-linked  
931 (lanes 1, 2, 4 and 5) or cross-linked (lanes 3, 6 and 7) samples in SDS-PAGE sample buffer at 37°C  
932 for 10 minutes (lanes 1, 3, 4 and 6) or at 95°C for 30 min in the presence of 10 mM dithiothreitol  
933 (lanes 2, 5 and 7).

934 B. Lipomodified PrsA-Myc in *B. subtilis* IH8478 cross-linked and heated at 37°C for 10 min (lane  
935 1) or at 95°C for 30 min (lane 3). Corresponding samples from *B. subtilis* RH2111, the parental  
936 strain not expressing PrsA-Myc, were used as negative controls (lanes 2 and 4, respectively).

937

938

939 **ACKNOWLEDGEMENTS**

940

941 This work, as part of the European Science Foundation EUROCORES Programme EuroSCOPE is  
942 supported by funds from the European Commission's Sixth Framework Programme under contract  
943 ERAS-CT-2003-980409. The work was also supported from the grants 107438, 113846 and 123318  
944 from the Academy of Finland. BCM was supported by a grant from ALW-NWO in the Bacell  
945 SysMO programma.

946

947 We would like to thank the Department of Molecular Cell Biology of the University of Groningen,  
948 the Netherlands, for giving access to microscopy facilities and A. M. Krikken for fluorescence  
949 microscopy support. We want to thank David Popham (Virginia Tech) and Mark Leaver (Newcastle  
950 University) for several PBP mutants and gene constructs. We are also grateful to Sanna Marjavaara  
951 (University of Helsinki) for assistance in image acquisition and quantitation of Bocillin-FL-labeled  
952 samples.

953

954 **REFERENCES**

955

956 Alonzo, F., 3rd, Port, G. C., Cao, M., and Freitag, N. E. (2009) The posttranslocation chaperone  
957 PrsA2 contributes to multiple facets of *Listeria monocytogenes* pathogenesis. *Infect Immun*  
958 **77**: 2612-2623.

959 Antelmann, H., Darmon, E., Noone, D., Veening, J. W., Westers, H., Bron, S., et al. (2003) The  
960 extracellular proteome of *Bacillus subtilis* under secretion stress conditions. *Mol Microbiol*  
961 **49**: 143-156.

962 Atrih, A., Bacher, G., Allmaier, G., Williamson, M. P., and Foster, S. J. (1999) Analysis of  
963 peptidoglycan structure from vegetative cells of *Bacillus subtilis* 168 and role of PBP 5 in  
964 peptidoglycan maturation. *J Bacteriol* **181**: 3956-3966.

965 Behrens, S., Maier, R., de Cock, H., Schmid, F. X., and Gross, C. A. (2001) The SurA periplasmic  
966 PPIase lacking its parvulin domains functions in vivo and has chaperone activity. *EMBO J*  
967 **20**: 285-294.

968 Bramkamp, M., Weston, L., Daniel, R. A., and Errington, J. (2006) Regulated intramembrane  
969 proteolysis of FtsL protein and the control of cell division in *Bacillus subtilis*. *Mol.*  
970 *Microbiol.* **62**: 580-591.

971 Carballido-Lopez, R., and Errington, J. (2003) The bacterial cytoskeleton: *in vivo* dynamics of the  
972 actin-like protein Mbl of *Bacillus subtilis*. *Dev Cell* **4**: 19-28.

973 Carballido-Lopez, R., Formstone, A., Li, Y., Ehrlich, S. D., Noirot, P., and Errington, J. (2006)  
974 Actin homolog MreBH governs cell morphogenesis by localization of the cell wall  
975 hydrolase LytE. *Dev Cell* **11**: 399-409.

976 Claessen, D., Emmins, R., Hamoen, L. W., Daniel, R. A., Errington, J., and Edwards, D. H. (2008)  
977 Control of the cell elongation-division cycle by shuttling of PBP1 protein in *Bacillus*  
978 *subtilis*. *Mol Microbiol* **68**: 1029-1046.

- 979 Courtin, P., Miranda, G., Guillot, A., Wessner, F., Mezange, C., Domakova, E., et al. (2006)  
980 Peptidoglycan structure analysis of *Lactococcus lactis* reveals the presence of an L,D-  
981 carboxypeptidase involved in peptidoglycan maturation. *J Bacteriol* **188**: 5293-5298.
- 982 Daniel, R. A., and Errington, J. (2003) Control of cell morphogenesis in bacteria: two distinct ways  
983 to make a rod-shaped cell. *Cell* **113**: 767-776.
- 984 Daniel, R. A., Harry, E. J., Katis, V. L., Wake, R. G., and Errington, J. (1998) Characterization of  
985 the essential cell division gene *ftsL(yIID)* of *Bacillus subtilis* and its role in the assembly of  
986 the division apparatus. *Mol Microbiol* **29**: 593-604.
- 987 Daniel, R. A., Noirot-Gros, M. F., Noirot, P., and Errington, J. (2006) Multiple interactions between  
988 the transmembrane division proteins of *Bacillus subtilis* and the role of FtsL instability in  
989 divisome assembly. *J Bacteriol* **188**: 7396-7404.
- 990 Darmon, E., Noone, D., Masson, A., Bron, S., Kuipers, O. P., Devine, K. M., and van Dijl, J. M.  
991 (2002) A novel class of heat and secretion stress-responsive genes is controlled by the  
992 autoregulated CssRS two-component system of *Bacillus subtilis*. *J Bacteriol* **184**: 5661-  
993 5671.
- 994 Defeu Soufo, H. J., and Graumann, P. L. (2004) Dynamic movement of actin-like proteins within  
995 bacterial cells. *EMBO Rep* **5**: 789-794.
- 996 Defeu Soufo, H. J., and Graumann, P. L. (2006) Dynamic localization and interaction with other  
997 *Bacillus subtilis* actin-like proteins are important for the function of MreB. *Mol Microbiol*  
998 **62**: 1340-1356.
- 999 Divakaruni, A. V., Baida, C., White, C. L., and Gober, J. W. (2007) The cell shape proteins MreB  
1000 and MreC control cell morphogenesis by positioning cell wall synthetic complexes. *Mol*  
1001 *Microbiol* **66**: 174-188.

- 1002 Divakaruni, A. V., Loo, R. R., Xie, Y., Loo, J. A., and Gober, J. W. (2005) The cell-shape protein  
1003 MreC interacts with extracytoplasmic proteins including cell wall assembly complexes in  
1004 *Caulobacter crescentus*. *Proc Natl Acad Sci U S A* **102**: 18602-18607.
- 1005 Drouault, S., Anba, J., Bonneau, S., Bolotin, A., Ehrlich, S. D., and Renault, P. (2002) The  
1006 peptidyl-prolyl isomerase motif is lacking in PmpA, the PrsA-like protein involved in the  
1007 secretion machinery of *Lactococcus lactis*. *Appl Environ Microbiol* **68**: 3932-3942.
- 1008 Ellermeier, C. D., and Losick, R. (2006) Evidence for a novel protease governing regulated  
1009 intramembrane proteolysis and resistance to antimicrobial peptides in *Bacillus subtilis*.  
1010 *Genes Dev* **20**: 1911-1922.
- 1011 Eymann, C., Dreisbach, A., Albrecht, D., Bernhardt, J., Becher, D., Gentner, S., et al. (2004) A  
1012 comprehensive proteome map of growing *Bacillus subtilis* cells. *Proteomics* **4**: 2849-2876.
- 1013 Figge, R. M., Divakaruni, A. V., and Gober, J. W. (2004) MreB, the cell shape-determining  
1014 bacterial actin homologue, co-ordinates cell wall morphogenesis in *Caulobacter crescentus*.  
1015 *Mol Microbiol* **51**: 1321-1332.
- 1016 Formstone, A., and Errington, J. (2005) A magnesium-dependent mreB null mutant: implications  
1017 for the role of mreB in *Bacillus subtilis*. *Mol Microbiol* **55**: 1646-1657.
- 1018 Glauner, B. (1988) Separation and quantification of muropeptides with high-performance liquid  
1019 chromatography. *Anal Biochem* **172**: 451-464.
- 1020 Glauner, B., Holtje, J. V., and Schwarz, U. (1988) The composition of the murein of *Escherichia*  
1021 *coli*. *J Biol Chem* **263**: 10088-10095.
- 1022 Hani, J., Schelbert, B., Bernhardt, A., Domdey, H., Fischer, G., Wiebauer, K., and Rahfeld, J. U.  
1023 (1999) Mutations in a peptidylprolyl-*cis/trans*-isomerase gene lead to a defect in 3'-end  
1024 formation of a pre-mRNA in *Saccharomyces cerevisiae*. *J Biol Chem* **274**: 108-116.
- 1025 Harry, E. J., Pogliano, K., and Losick, R. (1995) Use of immunofluorescence to visualize cell-  
1026 specific gene expression during sporulation in *Bacillus subtilis*. *J Bacteriol* **177**: 3386-3393.

- 1027 Healy, J., Weir, J., Smith, I., and Losick, R. (1991) Post-transcriptional control of a sporulation  
1028 regulatory gene encoding transcription factor sigma H in *Bacillus subtilis*. *Mol Microbiol* **5**:  
1029 477-487.
- 1030 Heikkinen, O., Seppala, R., Tossavainen, H., Heikkinen, S., Koskela, H., Permi, P., and  
1031 Kilpelainen, I. (2009) Solution structure of the parvulin-type PPIase domain of  
1032 *Staphylococcus aureus* PrsA--implications for the catalytic mechanism of parvulins. *BMC*  
1033 *Struct Biol* **9**: 17.
- 1034 Heinrich, J., Lunden, T., Kontinen, V. P., and Wiegert, T. (2008) The *Bacillus subtilis* ABC  
1035 transporter EcsAB influences intramembrane proteolysis through RasP. *Microbiology* **154**:  
1036 1989-1997.
- 1037 Hennecke, G., Nolte, J., Volkmer-Engert, R., Schneider-Mergener, J., and Behrens, S. (2005) The  
1038 periplasmic chaperone SurA exploits two features characteristic of integral outer membrane  
1039 proteins for selective substrate recognition. *J Biol Chem* **280**: 23540-23548.
- 1040 Hyyryläinen, H. L., Sarvas, M., and Kontinen, V. P. (2005) Transcriptome analysis of the secretion  
1041 stress response of *Bacillus subtilis*. *Appl Microbiol Biotechnol* **67**: 389-396.
- 1042 Hyyryläinen, H.-L., Vitikainen, M., Thwaite, J., Wu, H., Sarvas, M., Harwood, C., et al. (2000) D-  
1043 alanine substitution of teichoic acids as a modulator of protein folding and stability at the  
1044 cytoplasmic membrane/cell wall interface of *Bacillus subtilis*. *J Biol Chem* **275**: 26696 -  
1045 26703.
- 1046 Hyyryläinen, H. L., Bolhuis, A., Darmon, E., Muukkonen, L., Koski, P., Vitikainen, M., et al.  
1047 (2001) A novel two-component regulatory system in *Bacillus subtilis* for the survival of  
1048 severe secretion stress. *Mol Microbiol* **41**: 1159-1172.
- 1049 Jacobs, M., Andersen, J. B., Kontinen, V., and Sarvas, M. (1993) *Bacillus subtilis* PrsA is required  
1050 *in vivo* as an extracytoplasmic chaperone for secretion of active enzymes synthesized either  
1051 with or without pro-sequences. *Mol Microbiol* **8**: 957-966.

- 1052 Jensen, S. O., Thompson, L. S., and Harry, E. J. (2005) Cell division in *Bacillus subtilis*: FtsZ and  
1053 FtsA association is Z-ring independent, and FtsA is required for efficient midcell Z-Ring  
1054 assembly. *J Bacteriol* **187**: 6536-6544.
- 1055 Jones, L. J., Carballido-Lopez, R., and Errington, J. (2001) Control of cell shape in bacteria: helical,  
1056 actin-like filaments in *Bacillus subtilis*. *Cell* **104**: 913-922.
- 1057 Kalinowski, J., Bathe, B., Bartels, D., Bischoff, N., Bott, M., Burkovski, A., et al. (2003) The  
1058 complete *Corynebacterium glutamicum* ATCC 13032 genome sequence and its impact on  
1059 the production of L-aspartate-derived amino acids and vitamins. *J Biotechnol* **104**: 5-25.
- 1060 Kaltwasser, M., Wiegert, T., and Schumann, W. (2002) Construction and application of epitope-  
1061 and green fluorescent protein-tagging integration vectors for *Bacillus subtilis*. *Appl Environ*  
1062 *Microbiol* **68**: 2624-2628.
- 1063 Katis, V. L., and Wake, R. G. (1999) Membrane-bound division proteins DivIB and DivIC of  
1064 *Bacillus subtilis* function solely through their external domains in both vegetative and  
1065 sporulation division. *J Bacteriol* **181**: 2710-2718.
- 1066 Kawai, Y., Daniel, R. A., and Errington, J. (2009) Regulation of cell wall morphogenesis in  
1067 *Bacillus subtilis* by recruitment of PBP1 to the MreB helix. *Mol Microbiol* **71**: 1131-1144.
- 1068 Kontinen, V., and Sarvas, M. (1993) The PrsA lipoprotein is essential for protein secretion in  
1069 *Bacillus subtilis* and sets a limit for high-level secretion. *Mol Microbiol* **8**: 727-737.
- 1070 Kunst, F., Ogasawara, N., Moszer, I., Albertini, A. M., Alloni, G., Azevedo, V., et al. (1997) The  
1071 complete genome sequence of the gram-positive bacterium *Bacillus subtilis*. *Nature* **390**:  
1072 249-256.
- 1073 Leaver, M., and Errington, J. (2005) Roles for MreC and MreD proteins in helical growth of the  
1074 cylindrical cell wall in *Bacillus subtilis*. *Mol Microbiol* **57**: 1196-1209.

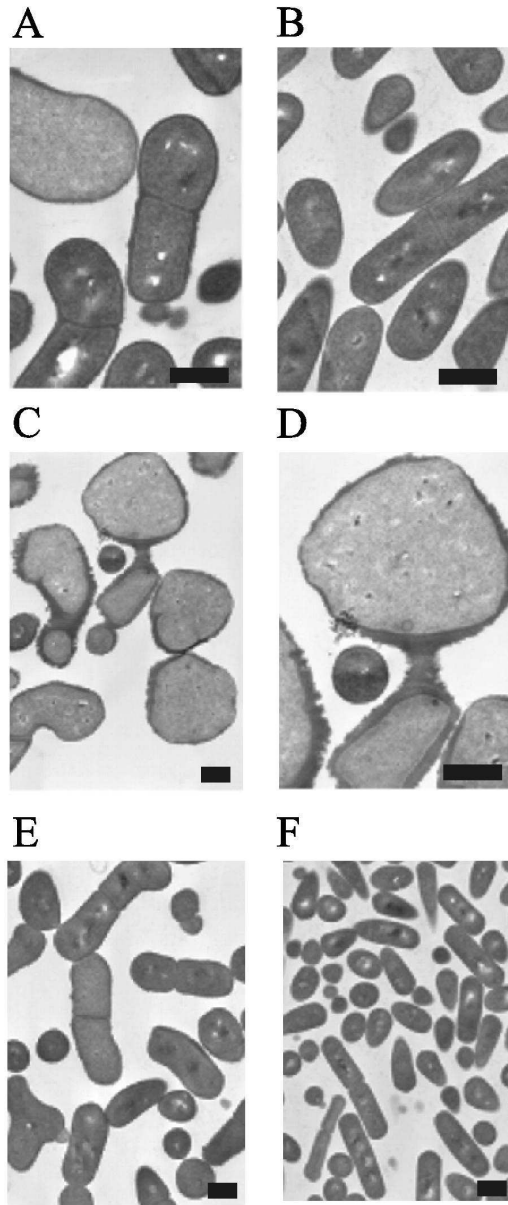
- 1075 Letek, M., Ordonez, E., Vaquera, J., Margolin, W., Flardh, K., Mateos, L. M., and Gil, J. A. (2008)  
1076 DivIVA is required for polar growth in the MreB-lacking rod-shaped actinomycete  
1077 *Corynebacterium glutamicum*. *J Bacteriol* **190**: 3283-3292.
- 1078 Lindholm, A., Ellmen, U., Tolonen-Martikainen, M., and Palva, A. (2006) Heterologous protein  
1079 secretion in *Lactococcus lactis* is enhanced by the *Bacillus subtilis* chaperone-like protein  
1080 PrsA. *Appl Microbiol Biotechnol* **73**: 904-914.
- 1081 Lu, K. P., Hanes, S. D., and Hunter, T. (1996) A human peptidyl-prolyl isomerase essential for  
1082 regulation of mitosis. *Nature* **380**: 544-547.
- 1083 Lu, K. P., and Zhou, X. Z. (2007) The prolyl isomerase PIN1: a pivotal new twist in  
1084 phosphorylation signalling and disease. *Nat Rev Mol Cell Biol* **8**: 904-916.
- 1085 Lu, P. J., Zhou, X. Z., Shen, M., and Lu, K. P. (1999) Function of WW domains as phosphoserine-  
1086 or phosphothreonine-binding modules. *Science* **283**: 1325-1328.
- 1087 Ma, Y., Bryant, A. E., Salmi, D. B., Hayes-Schroer, S. M., McIndoo, E., Aldape, M. J., and  
1088 Stevens, D. L. (2006) Identification and characterization of bicistronic *speB* and *prsA* gene  
1089 expression in the group A *Streptococcus*. *J Bacteriol* **188**: 7626-7634.
- 1090 Margot, P., and Karamata, D. (1996) The *wprA* gene of *Bacillus subtilis* 168, expressed during  
1091 exponential growth, encodes a cell-wall-associated protease. *Microbiology* **142**: 3437-3444.
- 1092 McPherson, D. C., Driks, A., and Popham, D. L. (2001) Two class A high-molecular-weight  
1093 penicillin-binding proteins of *Bacillus subtilis* play redundant roles in sporulation. *J*  
1094 *Bacteriol* **183**: 6046-6053.
- 1095 Pedersen, L. B., Angert, E. R., and Setlow, P. (1999) Septal localization of penicillin-binding  
1096 protein 1 in *Bacillus subtilis*. *J Bacteriol* **181**: 3201-3211.
- 1097 Pinho, M. G., and Errington, J. (2003) Dispersed mode of *Staphylococcus aureus* cell wall synthesis  
1098 in the absence of the division machinery. *Mol Microbiol* **50**: 871-881.

- 1099 Popham, D. L., Helin, J., Costello, C. E., and Setlow, P. (1996) Analysis of the peptidoglycan  
1100 structure of *Bacillus subtilis* endospores. *J Bacteriol* **178**: 6451-6458.
- 1101 Popham, D. L., and Setlow, P. (1995) Cloning, nucleotide sequence, and mutagenesis of the  
1102 *Bacillus subtilis ponA* operon, which codes for penicillin-binding protein (PBP) 1 and a  
1103 PBP-related factor. *J Bacteriol* **177**: 326-335.
- 1104 Popham, D. L., and Setlow, P. (1996) Phenotypes of *Bacillus subtilis* mutants lacking multiple class  
1105 a high-molecular-weight penicillin-binding proteins. *J Bacteriol* **178**: 2079-2085.
- 1106 Popham, D. L., and Young, K. D. (2003) Role of penicillin-binding proteins in bacterial cell  
1107 morphogenesis. *Curr Opin Microbiol* **6**: 594-599.
- 1108 Rahfeld, J.-U., Rücknagel, K. P., Schelbert, B., Ludvig, B., Hacker, J., Mann, K., and Fischer, G.  
1109 (1994) Confirmation of the existence of a third family among peptidyl-prolyl *cis/trans*  
1110 isomerases. Amino acid sequence and recombinant production of parvulin. *FEBS Lett* **352**:  
1111 180-184.
- 1112 Robson, S. A., and King, G. F. (2006) Domain architecture and structure of the bacterial cell  
1113 division protein DivIB. *Proc Natl Acad Sci U S A* **103**: 6700-6705.
- 1114 Rodgers, K. K., Bu, Z., Fleming, K. G., Schatz, D. G., Engelman, D. M., and Coleman, J. E. (1996)  
1115 A zinc-binding domain involved in the dimerization of RAG1. *J Mol Biol* **260**: 70-84.
- 1116 Sauvage, E., Kerff, F., Terrak, M., Ayala, J. A., and Charlier, P. (2008) The penicillin-binding  
1117 proteins: structure and role in peptidoglycan biosynthesis. *FEMS Microbiol Rev* **32**: 234-  
1118 258.
- 1119 Scheffers, D. J., Jones, L. J., and Errington, J. (2004) Several distinct localization patterns for  
1120 penicillin-binding proteins in *Bacillus subtilis*. *Mol Microbiol* **51**: 749-764.
- 1121 Schiene, C., and Fischer, G. (2000) Enzymes that catalyse the restructuring of proteins. *Curr Opin*  
1122 *Struct Biol* **10**: 40-45.

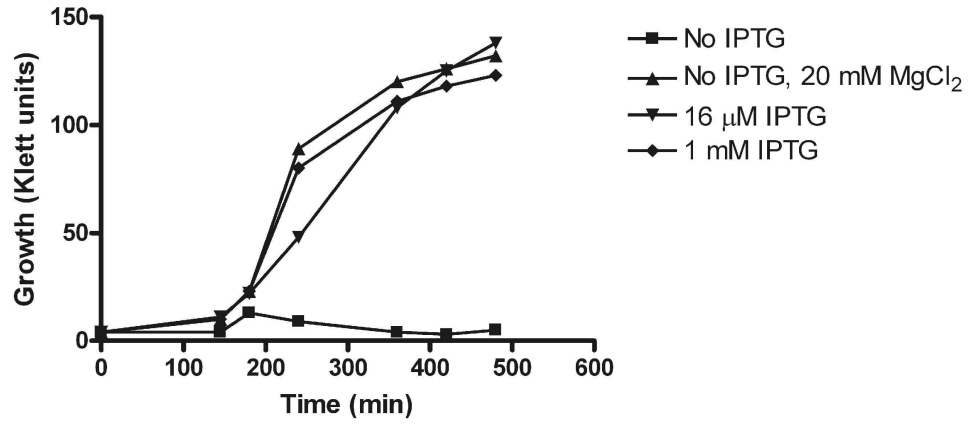
- 1123 Soufo, H. J., and Graumann, P. L. (2003) Actin-like proteins MreB and Mbl from *Bacillus subtilis*  
1124 are required for bipolar positioning of replication origins. *Curr Biol* **13**: 1916-1920.
- 1125 Spiess, C., Beil, A., and Ehrmann, M. (1999) A temperature-dependent switch from chaperone to  
1126 protease in a widely conserved heat shock protein. *Cell* **97**: 339-347.
- 1127 Stephenson, K., and Harwood, C. R. (1998) Influence of a cell-wall-associated protease on  
1128 production of  $\alpha$ -amylase by *Bacillus subtilis*. *Appl Environ Microbiol* **64**: 2875-2881.
- 1129 Stewart, G. C. (2005) Taking shape: control of bacterial cell wall biosynthesis. *Mol Microbiol* **57**:  
1130 1177-1181.
- 1131 Stulke, J., Hanschke, R., and Hecker, M. (1993) Temporal activation of beta-glucanase synthesis in  
1132 *Bacillus subtilis* is mediated by the GTP pool. *J Gen Microbiol* **139**: 2041-2045.
- 1133 Stymest, K. H., and Klappa, P. (2008) The periplasmic peptidyl prolyl *cis-trans* isomerases PpiD  
1134 and SurA have partially overlapping substrate specificities. *FEBS J* **275**: 3470-3479.
- 1135 Tiyanont, K., Doan, T., Lazarus, M. B., Fang, X., Rudner, D. Z., and Walker, S. (2006) Imaging  
1136 peptidoglycan biosynthesis in *Bacillus subtilis* with fluorescent antibiotics. *Proc Natl Acad*  
1137 *Sci U S A* **103**: 11033-11038.
- 1138 Uchida, T., Fujimori, F., Tradler, T., Fischer, G., and Rahfeld, J.-U. (1999) Identification and  
1139 characterization of a 14 kDa human protein as a novel parvulin like peptidyl-prolyl *cis/trans*  
1140 isomerase. *FEBS Lett* **446**: 278-282.
- 1141 Wahlstrom, E., Vitikainen, M., Kontinen, V. P., and Sarvas, M. (2003) The extracytoplasmic  
1142 folding factor PrsA is required for protein secretion only in the presence of the cell wall in  
1143 *Bacillus subtilis*. *Microbiology* **149**: 569-577.
- 1144 van den Ent, F., Leaver, M., Bendezu, F., Errington, J., de Boer, P., and Lowe, J. (2006) Dimeric  
1145 structure of the cell shape protein MreC and its functional implications. *Mol Microbiol* **62**:  
1146 1631-1642.
- 1147 Wang, P., and Heitman, J. (2005) The cyclophilins. *Genome Biol* **6**: 226.

- 1148 Wei, Y., Havasy, T., McPherson, D. C., and Popham, D. L. (2003) Rod shape determination by the  
1149 *Bacillus subtilis* class B penicillin-binding proteins encoded by *pbpA* and *pbpH*. *J Bacteriol*  
1150 **185**: 4717-4726.
- 1151 Williams, R. C., Rees, M. L., Jacobs, M. F., Pragai, Z., Thwaite, J. E., Baillie, L. W., et al. (2003)  
1152 Production of *Bacillus anthracis* protective antigen is dependent on the extracellular  
1153 chaperone, PrsA. *J Biol Chem* **278**: 18056-18062.
- 1154 Vitikainen, M., Hyyrylainen, H. L., Kivimaki, A., Kontinen, V. P., and Sarvas, M. (2005) Secretion  
1155 of heterologous proteins in *Bacillus subtilis* can be improved by engineering cell  
1156 components affecting post-translocational protein folding and degradation. *J Appl Microbiol*  
1157 **99**: 363-375.
- 1158 Vitikainen, M., Lappalainen, I., Seppala, R., Antelmann, H., Boer, H., Taira, S., et al. (2004)  
1159 Structure-function analysis of PrsA reveals roles for the parvulin-like and flanking N- and  
1160 C-terminal domains in protein folding and secretion in *Bacillus subtilis*. *J Biol Chem* **279**:  
1161 19302-19314.
- 1162 Vitikainen, M., Pummi, T., Airaksinen, U., Wu, H., Sarvas, M., and Kontinen, V. P. (2001)  
1163 Quantitation of the capacity of the secretion apparatus and requirement for PrsA in growth  
1164 and secretion of  $\alpha$ -amylase in *Bacillus subtilis*. *J Bacteriol* **183**: 1881-1890.
- 1165 Wu, S. C., Ye, R., Wu, X. C., Ng, S. C., and Wong, S. L. (1998) Enhanced secretory production of  
1166 a single-chain antibody fragment from *Bacillus subtilis* by coproduction of molecular  
1167 chaperones. *J Bacteriol* **180**: 2830-2835.
- 1168 Wu, X., Wilcox, C. B., Devasahayam, G., Hackett, R. L., Arevalo-Rodriguez, M., Cardenas, M. E.,  
1169 et al. (2000) The Ess1 prolyl isomerase is linked to chromatin remodeling complexes and  
1170 the general transcription machinery. *EMBO J* **19**: 3727-3738.

- 1171 Yaffe, M. B., Schutkowski, M., Shen, M., Zhou, X. Z., Stukenberg, P. T., Rahfeld, J. U., et al.  
1172 (1997) Sequence-specific and phosphorylation-dependent proline isomerization: a potential  
1173 mitotic regulatory mechanism. *Science* **278**: 1957-1960.
- 1174 Yao, J. L., Kops, O., Lu, P. J., and Lu, K. P. (2001) Functional conservation of phosphorylation-  
1175 specific prolyl isomerases in plants. *J Biol Chem* **276**: 13517-13523.
- 1176 Zemansky, J., Kline, B. C., Woodward, J. J., Leber, J. H., Marquis, H., and Portnoy, D. A. (2009)  
1177 Development of a mariner-based transposon and identification of *Listeria monocytogenes*  
1178 determinants, including the peptidyl-prolyl isomerase PrsA2, that contribute to its hemolytic  
1179 phenotype. *J Bacteriol* **191**: 3950-3964.
- 1180 Zhao, G., Meier, T. I., Kahl, S. D., Gee, K. R., and Blaszczyk, L. C. (1999) BOCILLIN FL, a  
1181 sensitive and commercially available reagent for detection of penicillin-binding proteins.  
1182 *Antimicrob Agents Chemother* **43**: 1124-1128.
- 1183
- 1184

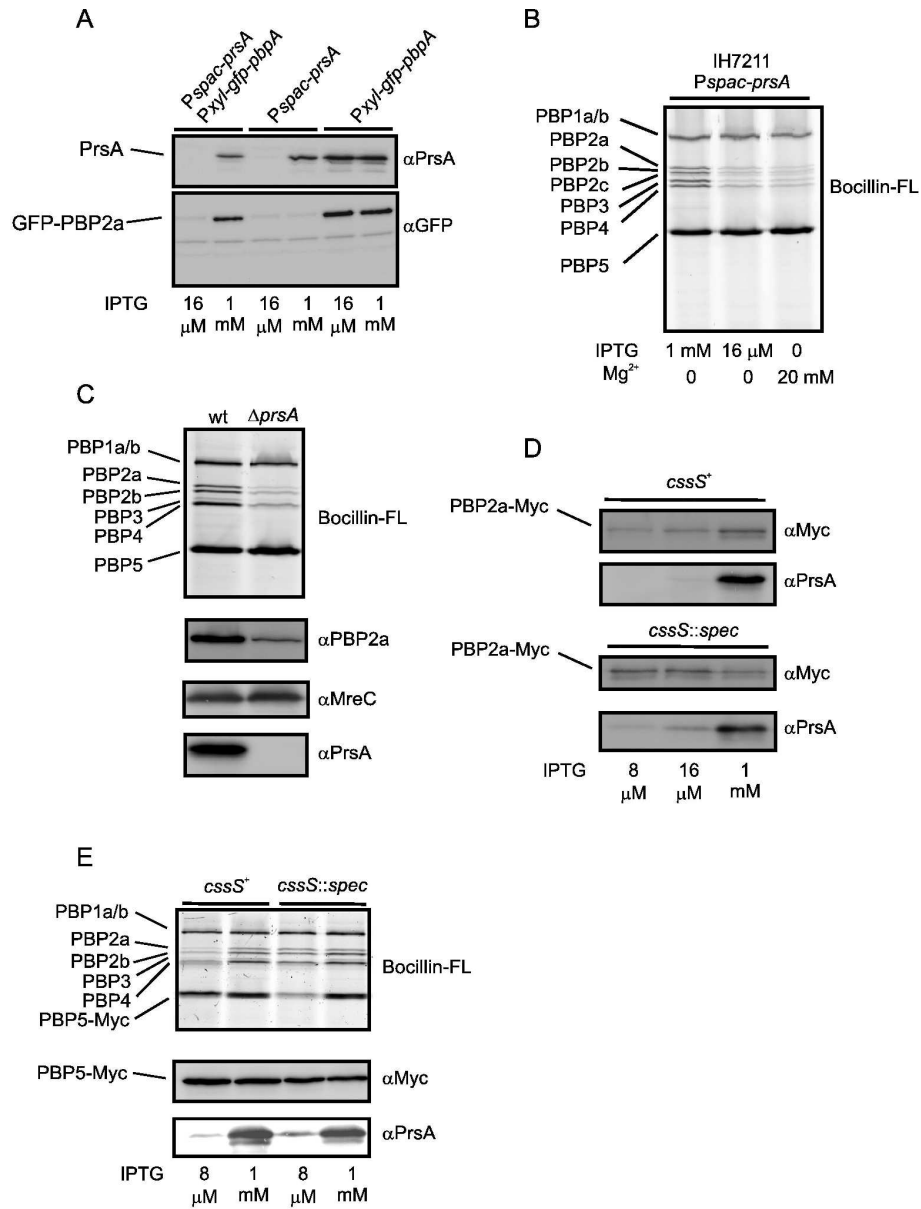


38x89mm (600 x 600 DPI)

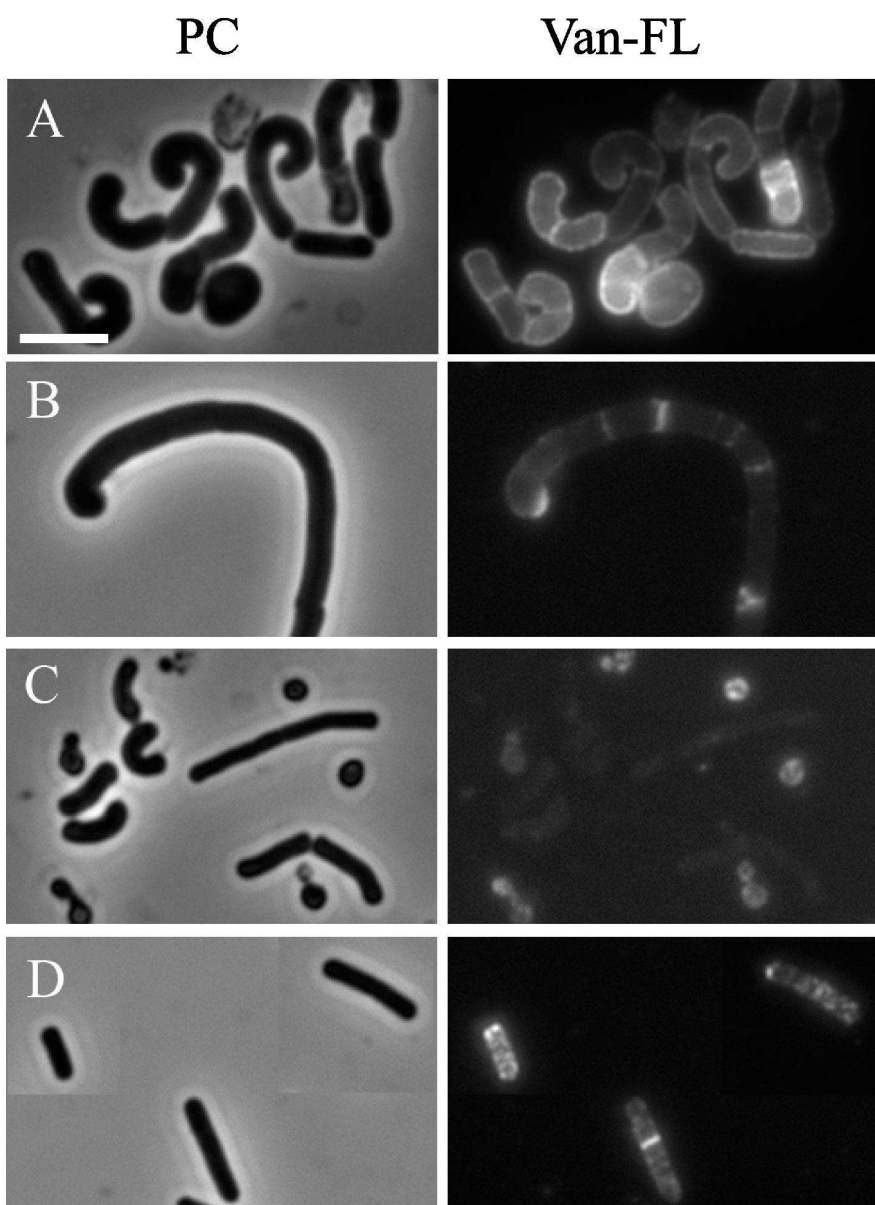


116x55mm (600 x 600 DPI)

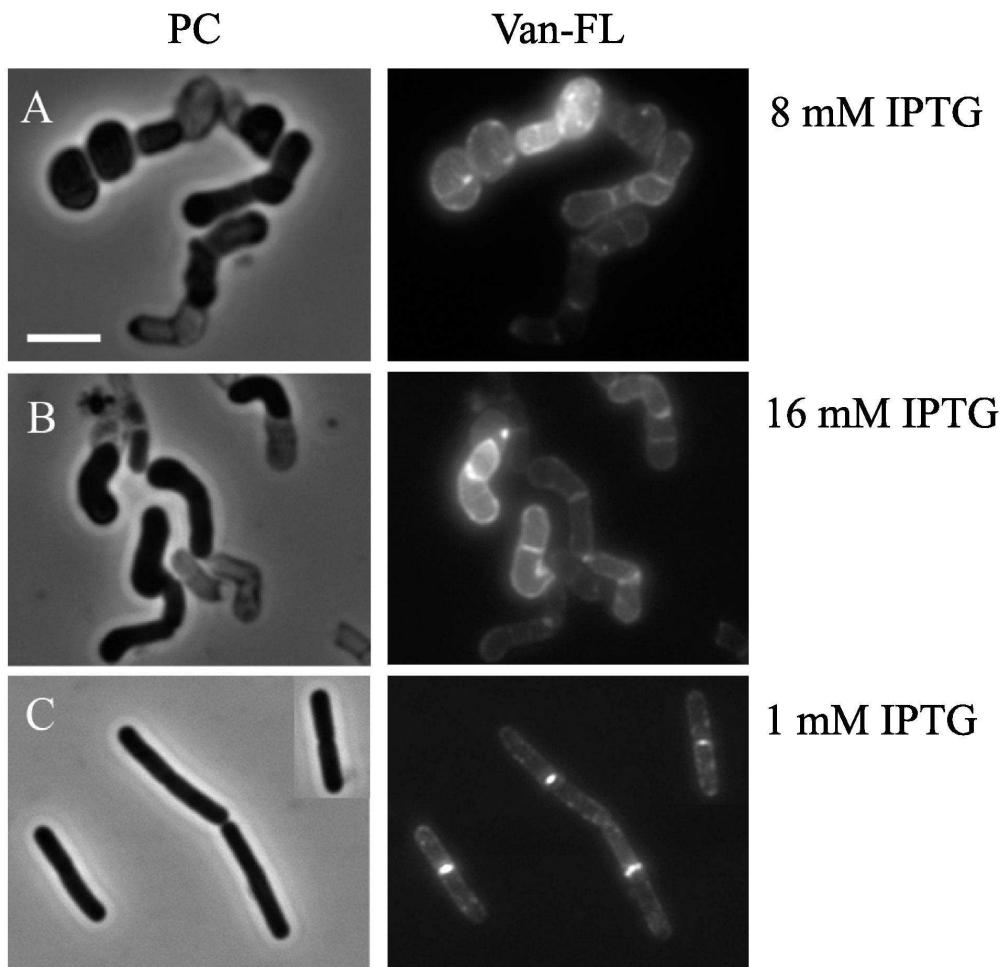
Peer Review



130x172mm (600 x 600 DPI)

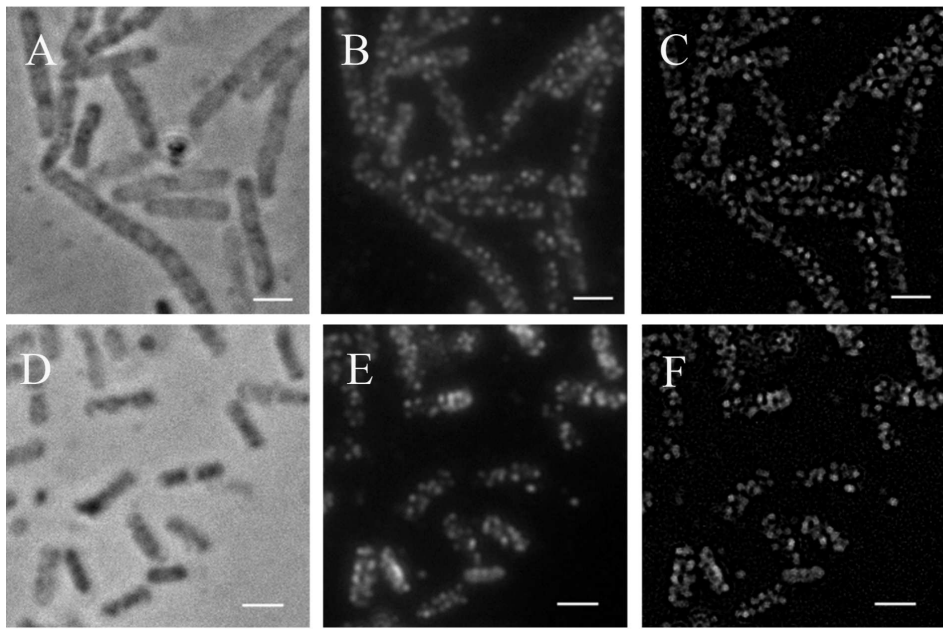
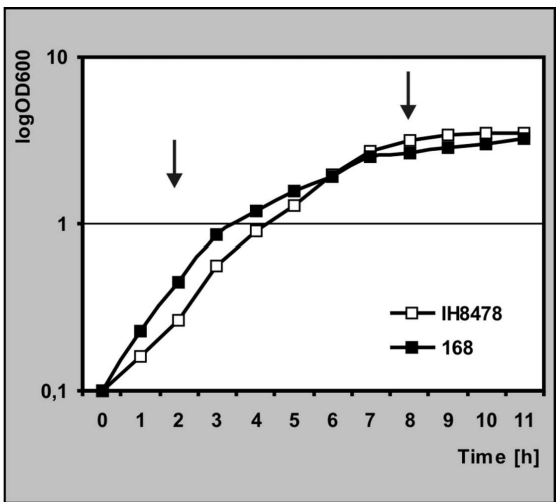


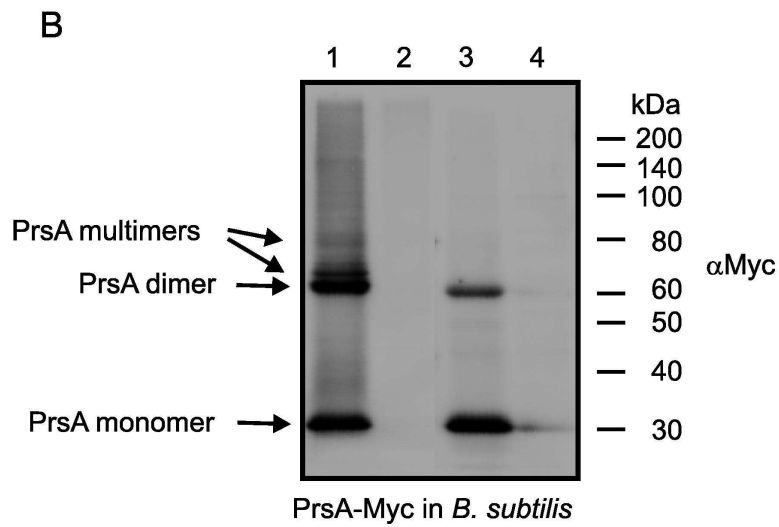
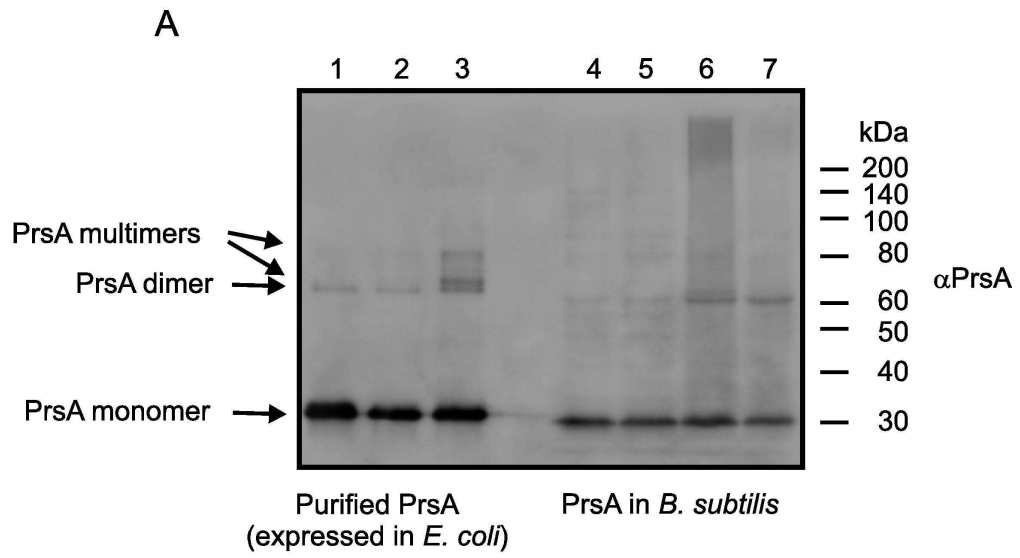
61x82mm (600 x 600 DPI)



80x77mm (600 x 600 DPI)







98x109mm (600 x 600 DPI)